

EUROPEAN SPACE AGENCY
CONTRACT REPORT

The work described in this report was done under ESA contract.
Responsibility for the contents resides in the author or organisation that prepared it.

Survey of Total Ionising Dose Tolerance of Power Bipolar Transistors and Silicon Carbide Devices for JUICE

TN6.5
SEE Test Report for
SiC Schottky Diode
SML020DH12

Manufacturer:
Semelab

Date code/Lot code: HM14070

Report no.	Version	Date	NEO no.
070/2018	1.0	2019-05-08	NEO-14-086
Author	Coauthors	Checked by	Project
Michael Steffens +49 2251 18-222 michael.steffens@int.fraunhofer.de	--	Stefan Höffgen	Survey of Total Ionising Dose Tolerance of Power Bipolar Transistors and Silicon Carbide Devices for JUICE (AO/1-7859/14/NL/SW)
Customer	Project management		
European Space Agency (ESA), contract number 4000113976/15/NL/RA	Project Coordinator: Stefan Höffgen (INT) ESA Technical Project Officer: Marc Poizat (ESA/ESTEC)		



Document Approval

Project	AO/1-8148/14/NL/SFe
Project Title	Survey of total ionising dose tolerance of power bipolar transistors and Silicon Carbide devices for JUICE
Doc ID	D6.5
Document Title	TN6.5 SEE Test Report for SiC Schottky Diode SML020DH12
Issue.Revision	0.1
Date	2019-03-15

Prepared by	
	Name: Michael Steffens, INT

Approved by	
	Name: Stefan Höffgen, INT

Accepted by	
	Name: Marc Poizat, ESTEC

Version history

Table 1: Revision history

Version	Date	Changed by	Changes
0.1	2019-03-15	Steffens	Initial draft, Sections 1-5, Appendices A+B
2.0	-	-	
	-	-	

Table of contents

Document Approval	2
1 Introduction	7
2 Summary	8
3 Sample preparations	11
4 Setup and Measurements	15
5 Tests at UCL	21
6 Tests at JULIC	27
7 Tests at GANIL	31
A Fraunhofer INT	34
B Appendix: Tests at UCL	37
C Appendix: Tests at JULIC	50
D Appendix: Tests at GANIL	55

List of figures

Figure 1: Safe operating voltage across the campaigns	9
Figure 2: Cross sections at $V_{GS} = 0$ V for each campaign	10
Figure 3: The ESD package with the samples	11
Figure 4: Sample marking	12
Figure 5: DUT decapsulation	13
Figure 6: Functional tests after parylene coating	13
Figure 7: Die pictures	14
Figure 8: Intended Test program	15
Figure 9: Detection Circuit	16
Figure 10: Test board layout	16
Figure 11: UCL: Measurement equipment/setup (including equipment for MOSFET/JFET tests) .	18
Figure 12: GANIL: Measurement equipment/setup (including equipment for MOSFET/JFET tests)	19
Figure 13: JULIC: Measurement equipment/setup (including equipment for MOSFET/JFET tests)	20
Figure 14: UCL vacuum chamber with electrical feedthroughs.	21
Figure 15: Plot of LETs and Ranges in Silicon Carbide at UCL.	23
Figure 16: Overview of results: Heavy Ions at UCL.....	25
Figure 17: Beam line and irradiation site at the JULIC injector cyclotron, FZ Jülich	27
Figure 18: Schematic setup of the beam exit window at JULIC and the ionization chamber.....	28
Figure 19: The initial proton energy	28
Figure 20: Overview of results: Protons at JULIC	30
Figure 21: Test setup at GANIL.....	31
Figure 22: Results: Protons at GANIL.	33
Figure 23: Run# 111, SML020DH12, Al-250, 7.1×10^4 ions/cm ² , DUT 16.2, $V_D = 600.0$ V.....	38
Figure 24: Run# 112, SML020DH12, Al-250, 1.0×10^5 ions/cm ² , DUT 15.1, $V_D = 500.0$ V.....	38
Figure 25: Run# 113, SML020DH12, Al-250, 1.0×10^5 ions/cm ² , DUT 15.1, $V_D = 550.0$ V.....	39
Figure 26: Run# 114, SML020DH12, Al-250, 2.1×10^5 ions/cm ² , DUT 15.1, $V_D = 550.0$ V.....	39
Figure 27: Run# 115, SML020DH12, Al-250, 3.1×10^5 ions/cm ² , DUT 15.2, $V_D = 550.0$ V.....	40
Figure 28: Run# 116, SML020DH12, C-131, 3.0×10^5 ions/cm ² , DUT 15.2, $V_D = 600.0$ V	40
Figure 29: Run# 117, SML020DH12, C-131, 3.1×10^5 ions/cm ² , DUT 15.2, $V_D = 750.0$ V	41
Figure 30: Run# 118, SML020DH12, C-131, 3.1×10^5 ions/cm ² , DUT 15.2, $V_D = 900.0$ V	41
Figure 31: Run# 119, SML020DH12, C-131, 3.1×10^5 ions/cm ² , DUT 15.2, $V_D = 1050.0$ V	42
Figure 32: Run# 120, SML020DH12, C-131, 3.1×10^5 ions/cm ² , DUT 15.2, $V_D = 1200.0$ V	42
Figure 33: Run# 121, SML020DH12, C-131, 3.1×10^5 ions/cm ² , DUT 16.1, $V_D = 1200.0$ V	43
Figure 34: Run# 122, SML020DH12, Kr-769, 1.0×10^5 ions/cm ² , DUT 16.1, $V_D = 100.0$ V	43
Figure 35: Run# 123, SML020DH12, Kr-769, 1.0×10^5 ions/cm ² , DUT 16.1, $V_D = 200.0$ V	44
Figure 36: Run# 124, SML020DH12, Kr-769, 1.0×10^5 ions/cm ² , DUT 16.1, $V_D = 300.0$ V	44
Figure 37: Run# 125, SML020DH12, Kr-769, 1.0×10^5 ions/cm ² , DUT 15.1, $V_D = 250.0$ V	45
Figure 38: Run# 126, SML020DH12, Kr-769, 2.1×10^5 ions/cm ² , DUT 15.1, $V_D = 250.0$ V	45
Figure 39: Run# 127, SML020DH12, Kr-769, 3.0×10^5 ions/cm ² , DUT 15.2, $V_D = 250.0$ V	46
Figure 40: Run# 128, SML020DH12, Cr-513, 1.0×10^5 ions/cm ² , DUT 20.1, $V_D = 300.0$ V	46
Figure 41: Run# 129, SML020DH12, Cr-513, 1.0×10^5 ions/cm ² , DUT 20.1, $V_D = 400.0$ V	47
Figure 42: Run# 130, SML020DH12, Cr-513, 1.0×10^5 ions/cm ² , DUT 20.2, $V_D = 350.0$ V	47
Figure 43: Run# 131, SML020DH12, Cr-513, 2.1×10^5 ions/cm ² , DUT 20.2, $V_D = 350.0$ V	48
Figure 44: Run# 132, SML020DH12, Cr-513, 3.1×10^5 ions/cm ² , DUT 17.1, $V_D = 300.0$ V	48
Figure 45: Run# 133, SML020DH12, Cr-513, 6.4×10^2 ions/cm ² , DUT 17.1, $V_D = 600.0$ V	49
Figure 46: Run# 042, SML020DH12, p, 1.1×10^{11} p/cm ² , DUT 1.1, $V_D = 1200.0$ V	53
Figure 47: Run# 043, SML020DH12, p, 1.1×10^{11} p/cm ² , DUT 1.2, $V_D = 1200.0$ V	53
Figure 48: Run# 044, SML020DH12, p, 1.1×10^{11} p/cm ² , DUT 2.1, $V_D = 1200.0$ V	54

Figure 49: SRIM2013 simulations of the Ganil Xenon tests on SiC	55
Figure 50: Run# 125, SML020DH12, Xe 0 mmAl, 150 mm Air, 6.0e+05 ions/cm ² , DUT 18.1, VD=250.0 V	57
Figure 51: Run# 126, SML020DH12, Xe 0 mmAl, 150 mm Air, 6.0e+05 ions/cm ² , DUT 18.1, VD=300.0 V	57
Figure 52: Run# 127, SML020DH12, Xe 0 mmAl, 150 mm Air, 6.0e+05 ions/cm ² , DUT 18.2, VD=250.0 V	58
Figure 53: Run# 128, SML020DH12, Xe 0 mmAl, 150 mm Air, 6.0e+05 ions/cm ² , DUT 19.1, VD=250.0 V	58
Figure 54: Run# 129, SML020DH12, Xe 400 mmAl, 95 mm Air, 6.0e+05 ions/cm ² , DUT 19.2, VD=200.0 V	59
Figure 55: Run# 130, SML020DH12, Xe 400 mmAl, 95 mm Air, 6.0e+05 ions/cm ² , DUT 19.2, VD=250.0 V	59
Figure 56: Run# 131, SML020DH12, Xe 400 mmAl, 95 mm Air, 6.0e+05 ions/cm ² , DUT 21.1, VD=200.0 V	60
Figure 57: Run# 132, SML020DH12, Xe 500 mmAl, 180 mm Air, 6.0e+05 ions/cm ² , DUT 21.1, VD=200.0 V	60
Figure 58: Run# 133, SML020DH12, Xe 500 mmAl, 180 mm Air, 6.0e+05 ions/cm ² , DUT 21.2, VD=150.0 V	61

List of tables

Table 1: Revision history	2
Table 2: Summary	8
Table 3: Sample shipment.....	11
Table 4: Sample marking:	12
Table 5: Measurement parameters.....	17
Table 6: UCL: Measurement equipment and instrumentation.....	18
Table 7: GANIL: Measurement equipment and instrumentation	19
Table 8: JULIC: Measurement equipment and instrumentation.....	19
Table 9: UCL: Ion energies, LETs and ranges in Silicon Carbide covered by 10 µm Parylene:	22
Table 10: UCL: Irradiation steps of SiC Schottky Diode SML020DH12.....	24
Table 11: Results: Heavy Ions at UCL - Calculated cross sections Calculated with the formulae in ESCC25100 with CL=0.95 and flux uncertainty of 10% (approx. worst case)	26
Table 12: Results of simulations of the LET with package thickness.	29
Table 13: JULIC: Irradiation steps of SiC Schottky Diode SML020DH12.....	30
Table 14: Results: Heavy Ions at UCL - Calculated cross sections Calculated with the formulae in ESCC25100 with CL=0.95 and flux uncertainty of 10% (approx. worst case)	30
Table 15: GANIL: Beam characteristics.....	32
Table 16: GANIL: Irradiation steps of SiC Schottky Diode SML020DH12.	32
Table 17: Results: Heavy Ions at GANIL - Calculated cross sections	33
Table 18: Mold material of example C2M0080120D. Values indicated with * are estimates.....	51
Table 19: Results of GRAS simulations of the LET with package thickness.....	51
Table 20: Intermediate results of MULASSIS simulations of the proton energy with package thickness.	51
Table 21: Results of SRIM simulations of the LET with package thickness.....	52
Table 22: GANIL: Beam characteristics.....	55

1 Introduction

1.1 Scope

The Fraunhofer Institute for Technological Trend Analysis (INT) carried out a series of Single Event Effects tests with protons and heavy ions on SiC Schottky Diode SML020DH12 from Semelab for the ESA project "Survey of Total Ionizing Dose Tolerance of Power Bipolar Transistors and Silicon Carbide Devices for JUICE" (ESA-TOPSIDE, AO/1-8148/14/NL/SFe) under contract number 4000113976/15/NL/RA.

This reports documents the preparation, execution and the results of these tests.

1.2 Applicable Documents

- [AD1] ITT/AO/1-8148/14/NL/SFe "Statement of work: Survey of Total Ionizing Dose Tolerance of Power Bipolar Transistors and Silicon Carbide Devices for JUICE"
- [AD2] Proposal for ITT/AO/1-8148/14/NL/SFe, Fraunhofer INT

1.3 Reference Documents

- [1] Website of Fraunhofer INT: <http://www.int.fraunhofer.de>
- [2] Guidelines for Evaluating and Expressing the Uncertainty of NIST Measurement Results, B.N. Taylor and C.E. Kuyatt, NIST Technical Note 1297, 1994, <http://www.nist.gov/pml/pubs/tn1297/index.cfm>.
- [3] ESCC Basic Specification No. 25100, issue 2, October 2014
- [4] Datasheet of SiC Schottky Diode SML020DH12, "SILICON CARBIDE POWER SCHOTTKY RECTIFIER DIODE SML020DH12", Semelab, Document Number 8960 Issue 2
- [5] TN3.5 "SEE (HI) Test Plan SML020DH12 (Schottky Diode)", Issue 1, Revision 4, 2018-04-15
- [6] TN3.11 "SEE (p) Test Plan SML020DH12 (Schottky Diode)", Issue 1 Revision 1, 2017-07-25
- [7] Casey et. al., "Schottky Diode Derating for Survivability in a Heavy Ion Environment", IEEE TNS vol. 62, no.6, pp. 2482-2489 (2015)
- [8] Website of the HIF Facility at UCL: <http://www.cyc.ucl.ac.be/HIF/HIF.php>, last accessed: 2019-01-17
- [9] SRIM 2013, www.srim.org, detailed in Ziegler et. Al., "SRIM - The stopping and range of ions in matter (2010)", Nuclear Instruments and Methods in Physics Research Section B, Volume 268, Issue 11-12, p. 1818-1823.016-12-08)
- [10] Website of SPENVIS, <https://www.spennis.oma.be/>
- [11] Website of the PSTAR database at NIST, <https://physics.nist.gov/PhysRefData/Star/Text/PSTAR.html>
- [12] Website of the GANIL facility for irradiation of electronic components: <https://www.ganil-spiral2.eu/en/industrial-users-2/applications-industrielles/irradiation-of-electronic-components/>

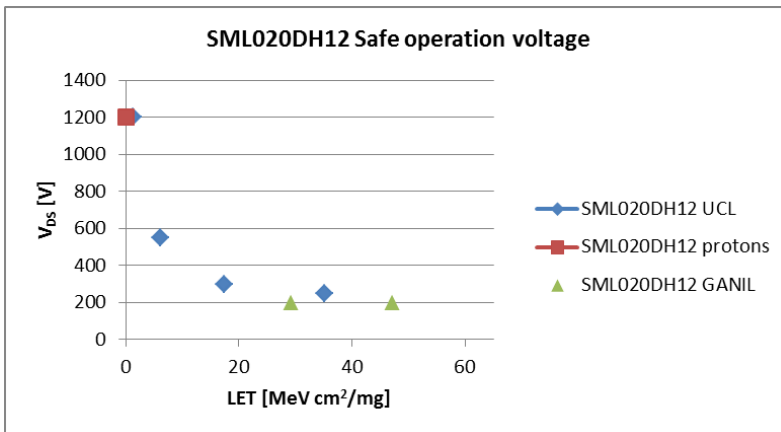
2 Summary

Table 2: Summary

Test Report Number	070/2018
Project (INT)	NEO-14-086
Customer	European Space Agency (ESA), contract number 4000113976/15/NL/RA
Contact	Project Coordinator: Stefan Höffgen (INT) ESA Technical Project Officer: Marc Poizat (ESA/ESTEC)
ESA project / contract number	AO/1-8148/14/NL/SFe 4000113976/15/NL/RA
Device under test	SML020DH12
Family	SiC Schottky Diode
Technology	SiC Power Schottky Rectifier Diode
Package	TO258 (TO-258AA)
Date code / Wafer lot	HM14070
SN	UCL: #15, #16, #17, #20 GANIL: #18, #19, #21 JULIC: #1, #2 (previously Gamma irradiated)
Manufacturer	Semelab
Irradiation test house	Fraunhofer INT
Radiation source	UCL and GANIL: Heavy Ions, JULIC: Protons
Irradiation facility	UCL, GANIL, JULIC
Generic specification	ESCC 25100 Iss. 2
Detail specification	MIL-STD-750-1 w/CHANGE 5, Method 1080.1
Test plan	TN3.5 "SEE (HI) Test Plan SML020DH12 (Schottky Diode)", Issue 1, Revision 4, 2018-04-15 TN3.11 "SEE (p) Test Plan SML020DH12 (Schottky Diode)", Issue 1 Revision 1, 2017-07-25
Single/Multiple Exposure	Multiple
Parameters tested	Reverse current
Dates	UCL: 2018-04-16 – 2018-04-17 GANIL: 2018-06-06 – 2018-06-07 JULIC: 2017-09-19 – 2017-09-20

2.1 Overview of results

Figure 1: Safe operating voltage across the campaigns



The heavy ion tests at UCL with the SiC Schottky Diode SML020DH12 were performed with 4 different LETs. To save some time, several runs were performed at a rather low total fluence of 1E5 ions/cm². However after a destructive event at some voltage a run to 3E5 ions/cm² was always performed to confirm the lower voltage level.

Considering the rather low number of devices, that number of LETs was only achievable by testing each of the two diodes per package separately, thus effectively doubling the number of available devices. We see no correlation that diode #2 in any package is more likely to fail if diode #1 already failed.

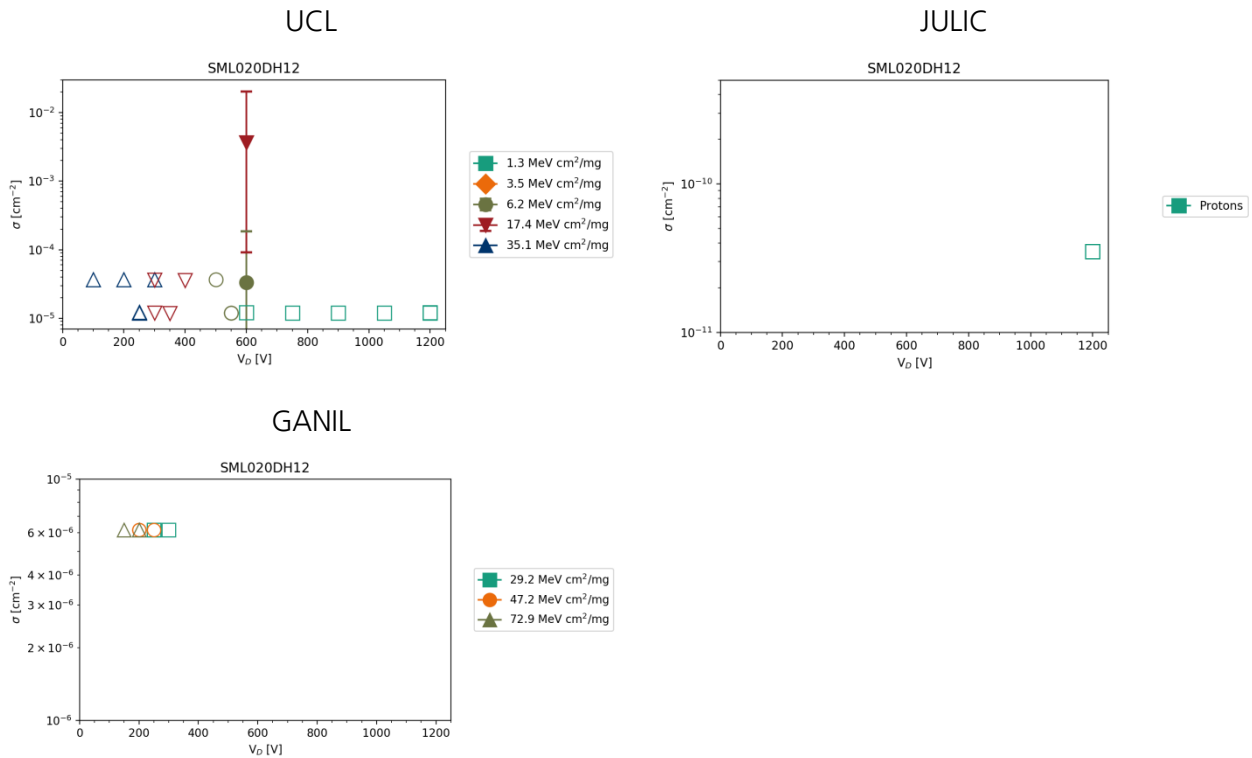
The voltage achievable for a safe operation up to the target fluence decreases from 1200 V with carbon ions (LET = 1.3 MeV cm²/mg) or protons down to 250 V with Krypton (LET = 35.1 MeV cm²/mg). LETs are given in SiC according to Table 9.

As indicated in the Figure 16 and Table 11, no immediate destructive event due to a single heavy ion was observed with Krypton up to a voltage of 300 V.

However at 300 V the leakage current showed a steady increase over approx. two orders of magnitude. This effect was not observed at 250 V and we therefore attribute that to be the safe operation voltage of this device at that LET.

The same effect was observed when irradiating with Chromium ions and the device at 400 V and to a lesser but similar extend at 350 V. We thus attribute 300 V to be the safe operation voltage of this device for the Chromium LET.

Figure 2: Cross sections at $V_{GS} = 0\text{ V}$ for each campaign Filled symbols mark the cross section in case of device failures and error bars mark the upper lower limits. Open symbols mark the cross section upper limit in case no failure was observed during a run.



After identifying the safe operation voltage for Chromium we performed another test at a deliberately much larger device voltage of 600 V to get an impression of the fluence-to-failure there. The device failed after less than 300 ions/cm² thus resulting in the remarkably large cross section in Figure 16.

From the tests at UCL we could already anticipate destructive effects at fairly low voltages with the LETs at GANIL. Thus in the tests at GANIL, the diode voltage was not increased beyond 250 V. No destructive events were observed, but a quasi-continuous degradation was already present.

2.2 Comments

- **All campaigns:**
 - Huge sensitivity in conjunction with a limited number of devices led to major deviations from the intended test plan.
 - Destructive events could not be mitigated.
- **Tests at JULIC:**
 - Test were performed with packaged DUTs.
 - Test devise were previously tested with Co-60 to 1 Mrad(Si).

3 Sample preparations

3.1 Sample shipment

A total of 30 Samples were procured by INT at a commercial supplier (Mouser Electronics) for the conduction of these tests for ESA. The parcel contained devices with one identification code (HM14070). The original package from Semelab indicates this as lot number.

Table 3: Sample shipment

Samples ordered	Samples received	Samples sent back
December 2015	December 2015	still at INT (partially used for other tests in this project)

Figure 3: The ESD package with the samples



3.2 Sample identification/ marking

The samples were soldered to adapter pins, to ease the mounting to the board, exchanging, plugging and storage of the samples.

The samples were colour marked to differentiate the samples between each other and to separate the samples of the different campaigns or types.

Figure 4: Sample marking



Table 4: Sample marking: Due to a limited number of samples, the DUTs tested with protons were previously used for a 1 Mrad(Si) TID campaign. Only DUTs used in the tests of this report are shown.

Condition	S/N	Color Code	Comment
UCL	15	[Red, Green, Blue]	decap, coated
	16	[Red, Blue, Purple]	decap, coated
	17	[Red, Black]	decap, coated
	20	[Red, Black]	decap, coated
GANIL	18	[Red, Grey]	decap, coated
	19	[Red, White]	decap, coated
	21	[Red, Red]	decap, coated
JULIC	1	[Red, Red]	non-decap, previously used for TID
	2	[Red, Red]	non-decap, previously used for TID

3.3 Sample decapsulation and preparation

In preparation for the heavy ion test campaign at UCL and GANIL, the DUTs were decapsulated and parylene coated. DUT decapsulation was performed at the mechanical workshop at INT by mechanically removing the lid of the devices (Figure 5). No filling mold was present, so removing the lid directly exposed the devices. We contacted the Semelab support and it was recommended to apply a Parylene coating to these devices.

Figure 5: DUT decapsulation. Batch of decapsulated SML020DH12



After decapsulation the functionality of all DUTs was checked. Due to the potentially missing insulation (inert gas) provided by the package, only tests at low voltage to prevent corona discharges were performed. All decapsulated devices passed these functional tests and 12 were sent for the coating process.

Parylene coating was performed by the “Advanced Chip & Wire Bonding” group, department “System Integration and Interconnection Technologies (SIIT)”, at Fraunhofer IZM in Berlin.

Tests of the reverse current performed at INT after receiving the coated samples, are shown in Figure 6. Two diodes are in each package and these were tested separately. One device (#23) did not pass this test. All others were considered for the SEE tests.

Figure 6: Functional tests after parylene coating

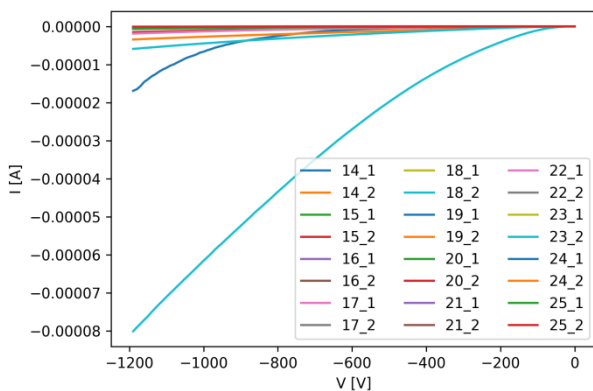
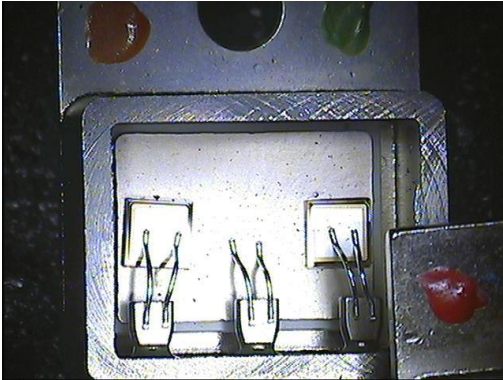
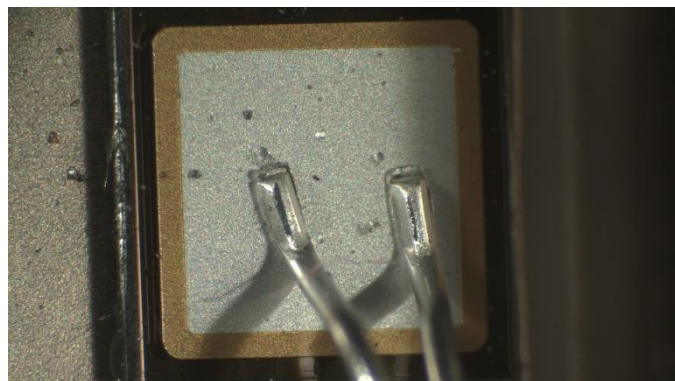
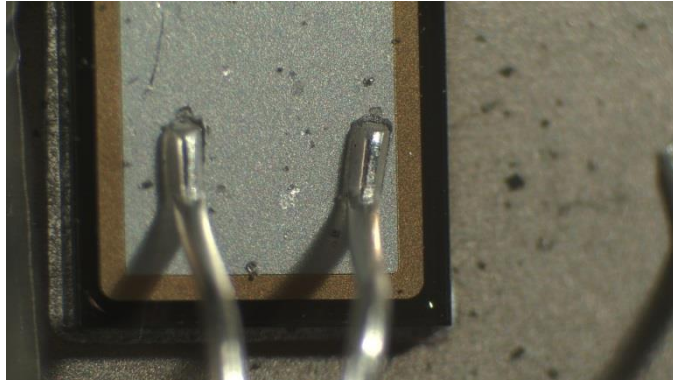


Figure 7: Die pictures. Images were taken with different optical microscopes. The camera used before the tests has a lower quality and resolution.



DUT #15 before tests at UCL



DUT #15 after tests at UCL (Top: left diode, bottom: right diode)

Figure 7 shows microscopic images of one DUT (#15) after parylene coating and after the tests at UCL wherein this DUT showed destructive failure. The surface of the DUT does not show signs indicating this destructive failure.

3.4 Sample safekeeping

The samples were stored in an Electro-Static Discharge (ESD) box (Figure 5) to handle them safely during the test, the interim storage after the last measurement and the final shipment.

4 Setup and Measurements

The test approach and setup covered in this section is mostly independent of the facility.

The tests performed with Heavy ions or protons aimed primarily at determining the safe operating voltage range rather than getting detailed cross sections for each setting and LET. This is mostly due to the high sensitivity of most of the SiC devices studied in this project to even moderate LETs.

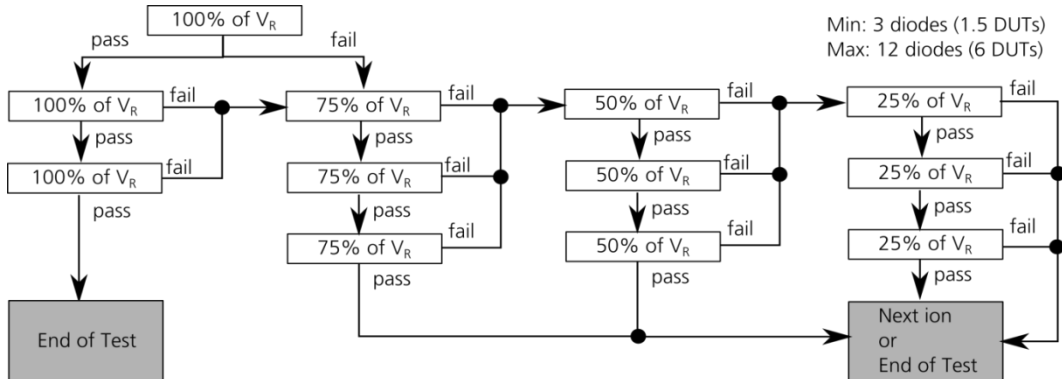
Due to a limited number of devices and having destructive failures which could not be mitigated, the required number of 3 samples to check the pass compliance of each test is not reached in any case.

4.1 Intended test program

The test logic is shown in Figure 8. As there are no applicable test standards or MIL test methods concerning Schottky diode SEE tests, the intended test logic follows mostly the approach for silicon Schottky diodes of Casey et. al. [7].

However during the tests and due to the high sensibility of the SiC diodes, this test program was in the end not followed.

Figure 8: Intended Test program



After each test step, a post-irradiation-stress-test is planned with the reverse voltage swept to its maximum rating.

4.2 Test Board and Detection Circuit

A custom-build printed-circuit board was manufactured to

- bias the samples according to the circuit-layout of the irradiation test plan [5] [6]
- fix the samples at the radiation source
- switch between the samples and connect the respectively active sample to the external setup
- detect destructive events

To reduce the number of parts required for testing, the two diodes in each DUT are biased separately (Figure 9). No mitigation of destructive events is foreseen.

Figure 9: Detection Circuit

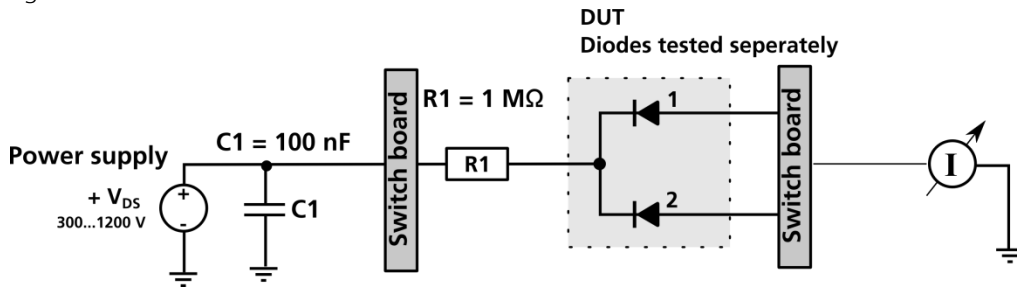
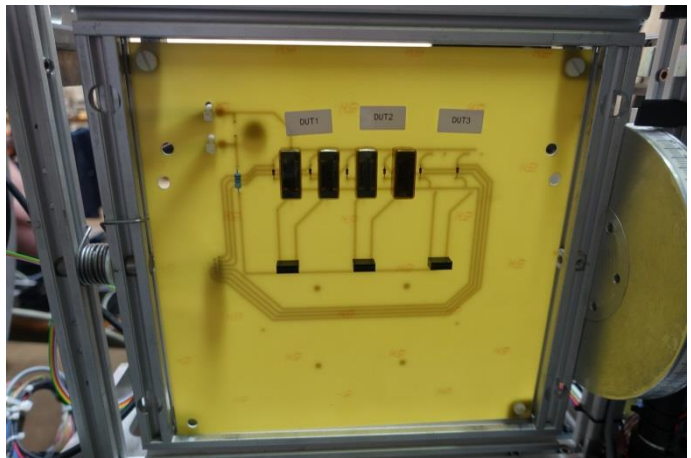
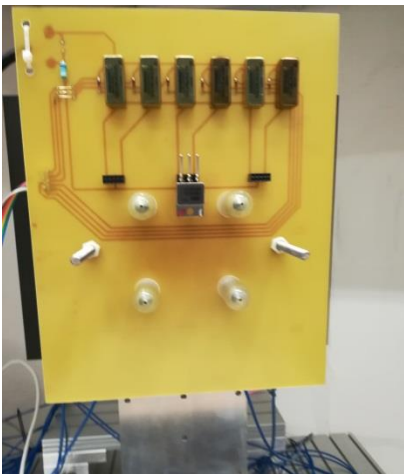
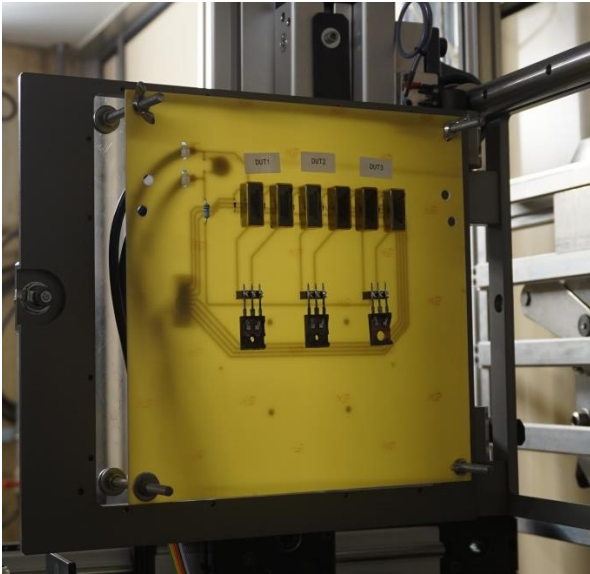


Figure 10: Test board layout Top left side: proton tests at JULIC, top right side: Heavy ion tests at UCL, bottom left: Heavy ion tests at GANIL





The boards used for the Heavy Ion and proton tests are functionally identical, but the proton board featured additional holes for four ionization chambers. The DUT was then positioned off-center from the beam, such that all ionization chambers and the DUT position are at the same distance from the center, thus allowing to calculate the proton flux at the DUT position without a fixed installation at the facility which would allow to do that. As a drawback, only one DUT position on the board could be used at a time.

For protons the board was at a distance of 1.8 m from the beam line exit window. Due to interaction in air and the exit window, the proton beam with initial energy 45 MeV was then broadened and reduced in energy to approx. 39 MeV.

The DUTs were exposed to the protons in package, thus when passing the package and hitting the sensitive volume of the devices, the proton energy is further reduced.

Calculations of the LETs in SiC are shown in the respective sections of the campaigns.

4.3 Measurement parameters

Parameters are continuously monitored during the runs. V_D is only indicated at the respective runs, I_D is shown in the appendices.

Table 5: Measurement parameters. Based on [4], taken from [5][6]

No.	Characteristics	Symbol	Remark
1	Reverse Voltage	V_D	Set according to test flow
2	Reverse Current	I_D	Monitored, typ. 10 μA @ 1200 V, max. 200 μA @ 1200 V

4.4 Measurement equipment

The test equipment is shown in Table 6 - Table 8 and Figure 11 - Figure 13.

The due date of the calibration can change from campaign to campaign if a new calibration was performed in the time between.

Table 6: UCL: Measurement equipment and instrumentation

Equipment	Manufacturer	Model	INT-Code	Calibr. due	Measurement
High Power System Source Meter	Keithley	2657A	E-SMU-012	03/2018	V_b, I_b
Data Acquisition/Switch unit	Agilent	34970A	E-SMF-002	n/a	Switch matrix
Triple Output Power Supply	Agilent	E3631A	E-PS3-002	n/a	Power supply of relays

Figure 11: UCL: Measurement equipment/setup (including equipment for MOSFET/JFET tests)

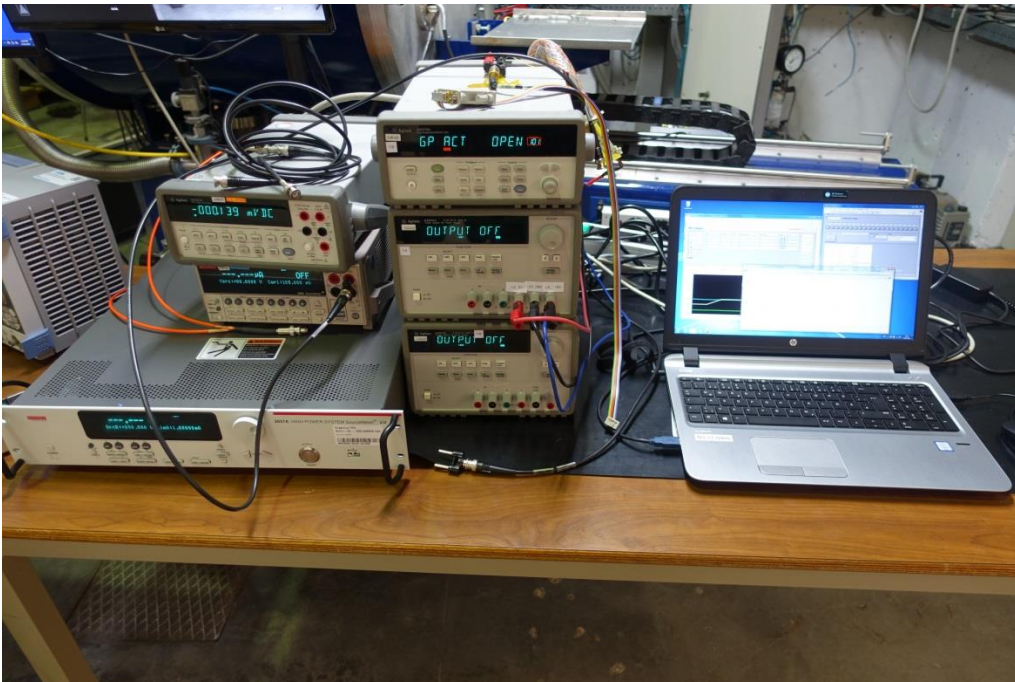


Table 7: GANIL: Measurement equipment and instrumentation

Equipment	Manufacturer	Model	INT-Code	Calibr. due	Measurement
High Power System Source Meter	Keithley	2657A	E-SMU-012	03/2020	V_D, I_D
Data Acquisition/Switch unit	Agilent	34970A	E-SMF-002	n/a	Switch matrix
Triple Output Power Supply	Agilent	E3631A	E-PS3-001	n/a	Power supply of of relais

Figure 12: GANIL: Measurement equipment/setup (including equipment for MOSFET/JFET tests)

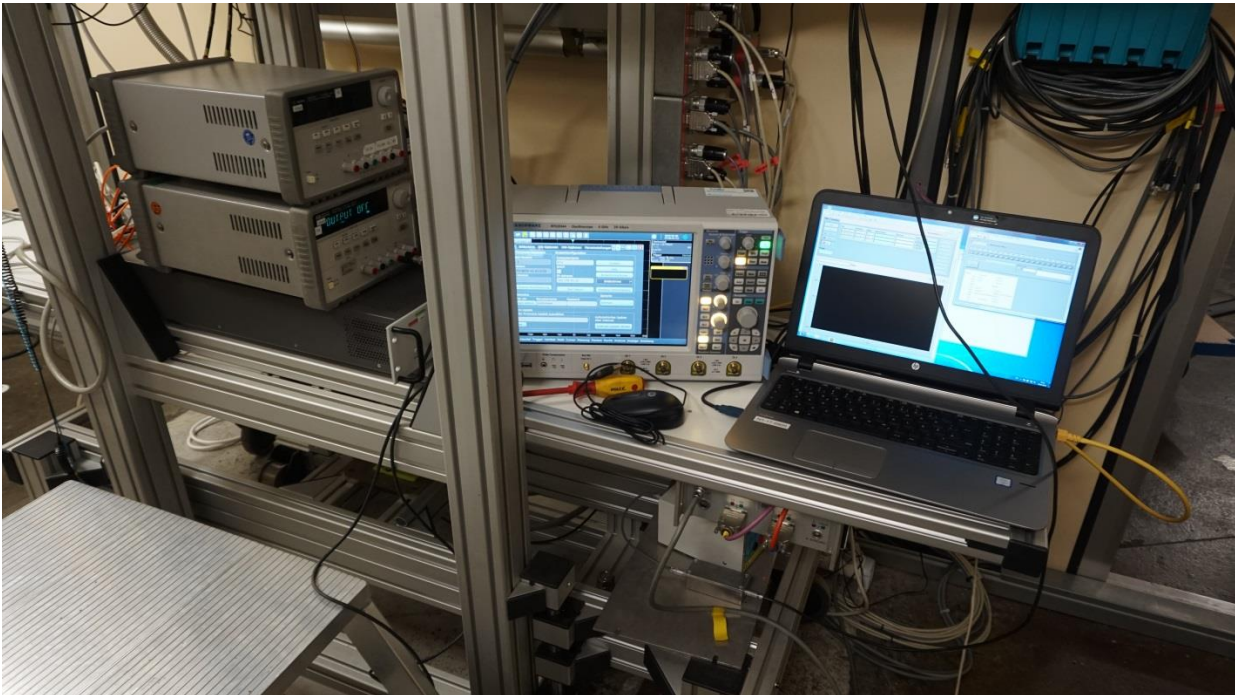
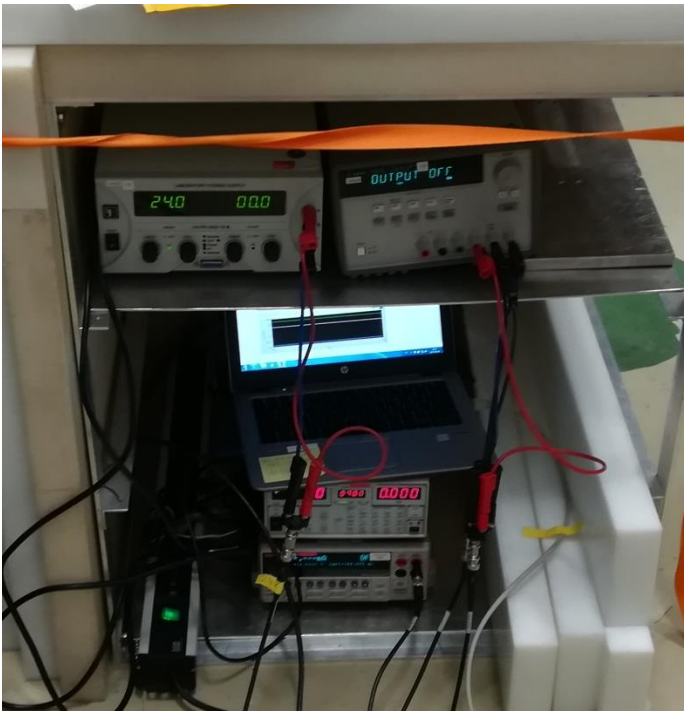


Table 8: JULIC: Measurement equipment and instrumentation

Equipment	Manufacturer	Model	INT-Code	Calibr. due	Measurement
5 kV Power supply	Keithley	2290E-5	E-PS1-030	10/2017	V_D, I_D
Laboratory Power Supply	EA	EA-PS-3032-10B	E-PS1-001	n/a	Control of relais

As only one DUT was on the board, no switch matrix was included in the setup, and the power supplies were only used to power the relays, not for switching between DUTs.

Figure 13: JULIC: Measurement equipment/setup (including equipment for MOSFET/JFET tests)



4.5 Measurement procedures

Bias conditions of diode were fixed for each step. When no destructive events occurred during a run, a post-irradiation-stress test was scheduled. In some instances across the campaigns, that POST test might not have been performed. These instances are commented in the respective sections.

5 Tests at UCL

5.1 Facility

The main heavy ion test was performed at the HIF facility of the CYCLONE cyclotron of the Université catholique de Louvain (UCL) in Louvain-la-Neuve.

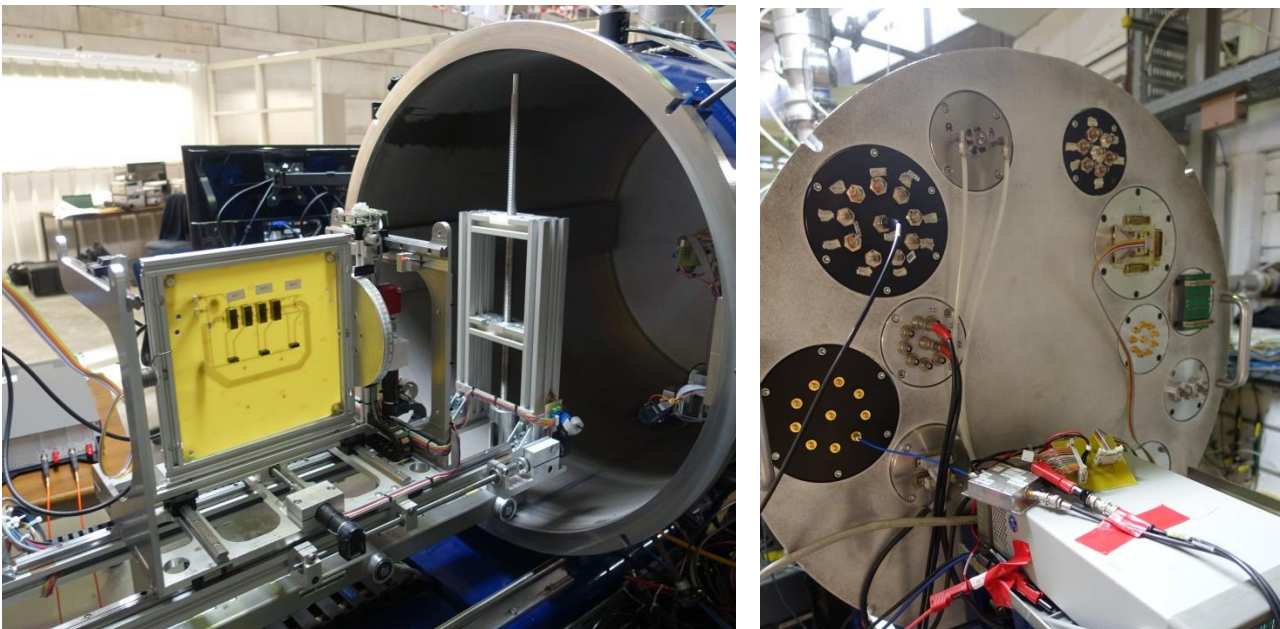
The facility can provide selected heavy ion beams from Carbon to Xenon in a particle cocktail with mass/charge ratio of approx. $M/Q=3.3$, allowing to switch from ion species to ion species quickly within the cocktail.

The experimental setup at the facility consists of the main vacuum chamber with a sample holder, which is moveable in x- and y-direction and can be tilted along one axis.

Feedthroughs can be used to connect boards within the enclosure with outside instrumentation (Figure 14).

Users can start and stop the irradiation from the user station next to the test chamber, other beam parameters like the particle flux can only be set by an operator.

Figure 14: UCL vacuum chamber with electrical feedthroughs. Two SHV cable feedthroughs, one DB9 feedthrough and one SMA feedthrough were used to connect the board with the outside instrumentation.



5.2 Beam parameters

The resulting total energies of the respective ions, as well as their LET and range in Silicon are provided by UCL [8]. However this data is not valid for Silicon Carbide.

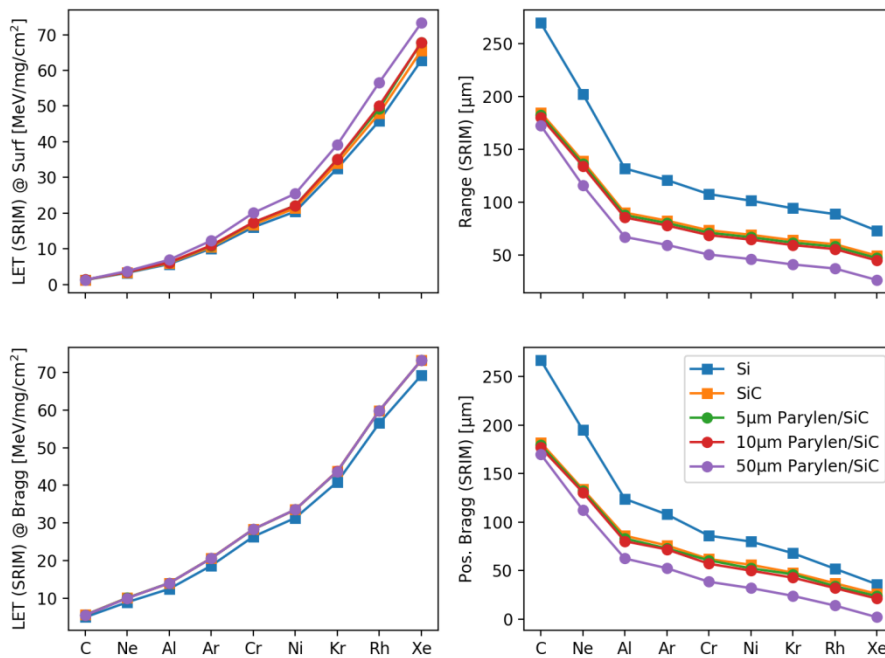
SRIM 2013 [9] simulations by Fraunhofer INT show the respective values for the heavy ion beams provided by UCL under normal incidence in Silicon Carbide covered by a 10 μm Parylene layer. Detailed data and a comparison to the data in blank Silicon Carbide is included in the test plan [5]. Tests with the SML020DH12 were only performed with ions marked in bold letters in Table 9.

Table 9: UCL: Ion energies, LETs and ranges in Silicon Carbide covered by 10 μm Parylene: Shown are the ions available at UCL [8]. LETs highlighted in bold font were actually used. LET and range data are based on SRIM2013 [9] simulations done at Fraunhofer INT.

Ion	Energy [MeV]	LET ^{SRIM} @ Surface [MeV cm ² /mg]	Range ^{SRIM*} [μm]	LET ^{SRIM} @ Bragg Peak [MeV cm ² /mg]	Depth of Bragg Peak* [μm]
C	131	1.33	180.22	5.49	176.90
Ne	238	3.49	134.13	10.02	130.70
Al	250	6.20	85.42	13.99	80.30
Ar	379	10.95	77.91	20.63	71.90
Cr	513	17.41	68.74	28.34	57.10
Ni	582	22.09	64.53	33.55	50.00
Kr	769	35.06	59.36	43.77	42.80
Rh	972	50.14	55.57	59.84	32.00
Xe	995	67.81	44.79	73.27	21.20

* Range and position of Bragg peak is given within the Silicon Carbide layer.

Figure 15: Plot of LETs and Ranges in Silicon Carbide at UCL. Additional data with Parylene layers and data for Silicon are included. Thin Parylene layers have limited impact.



5.3 Geometry

The board is attached to the moveable board holder (Figure 14) which can be fully retracted from the chamber for ease of access. Tests are then performed with the chamber sealed and evacuated.

5.4 Irradiation steps

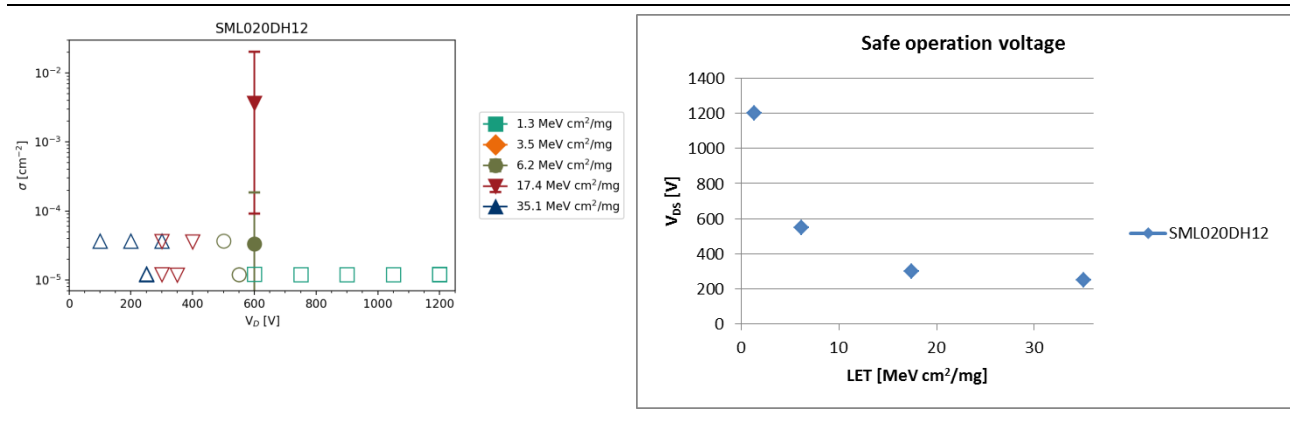
The log file of the tests performed at UCL can be found in Appendix B.B.1 shows an overview over the test indicating pass and fail results. A detailed evaluation of the results is shown in Section 7.3.

Table 10: UCL: Irradiation steps of SiC Schottky Diode SML020DH12. Numbers indicate the DUT serial number from Table 4. Table cells without numbers indicate that no run was performed under these conditions. Green or red background color indicate PASS or FAIL respectively. If a DUT fails at some voltage, all higher voltages are also indicated as fail. Yellow color (if applicable) indicates mixed results (e.g. 1 DUT passing, 1 DUT failing at the same level) or non-conclusive results with the device showing some damage not clearly attributable to a fail.

V _R [V]	C		Ne		Al		Cr		Kr	
	1.3		3.5		6.2		17.4		35.1	
	in-situ	Post	in-situ	Post	in-situ	Post	in-situ	Post	in-situ	Post
100									16.1	
200									16.1	
250									15.1, 15.2	
300							20.1, 17.1		16.1	
350							20.2			
400							20.1			
500					15.1					
550					15.1, 15.2					
600	15.2				16.2		17.1			
750	15.2									
900	15.2									
1050	15.2									
1200	15.2, 16.1									

5.5 Results

Figure 16: Overview of results: Heavy Ions at UCL. The left side image show the cross section results for various settings of V_D . Filled symbols mark the cross section in case of device failures and error bars mark the upper lower limits. Open symbols mark the cross section upper limit in case no failure was observed during a run. The right image shows the safe operating voltage.



The heavy ion tests at UCL with the SiC Schottky Diode SML020DH12 were performed with 4 different LETs. To save some time, several runs were performed at a rather low total fluence of 1E5 ions/cm². However after a destructive event at some voltage a run to 3E5 ions/cm² was always performed to confirm the lower voltage level.

A device which passes a run up to 3E5 ions/cm² without errors has an upper limit of the cross section of $\sigma_{upper} = 1.23E-5 \text{ cm}^2$ assuming 95%CL and 10% flux uncertainty.

Considering the rather low number of devices, that number of LETs was only achievable by testing each of the two diodes per package separately, thus effectively doubling the number of available devices. We see no correlation that diode #2 in any package is more likely to fail if diode #1 already failed.

The voltage achievable for a safe operation up to the target fluence decreases from 1200 V with carbon ions (LET = 1.3 MeV cm²/mg) down to 250 V with Krypton (LET = 35.1 MeV cm²/mg). LETs are given in SiC according to Table 9.

As indicated in the Figure 16 and Table 11, no immediate destructive event due to a single heavy ion was observed with Krypton up to a voltage of 300 V.

However at 300 V the leakage current showed a steady increase over approx. two orders of magnitude. This effect was not observed at 250 V and we therefore attribute that to be the safe operation voltage of this device at that LET.

The same effect was observed when irradiating with Chromium ions and the device at 400 V and to a lesser but similar extend at 350 V. We thus attribute 300 V to be the safe operation voltage of this device for the Chromium LET.

After identifying the safe operation voltage for Chromium we performed another test at a deliberately much larger device voltage of 600 V to get an impression of the fluence-to-failure there. The device failed after less than 300 ions/cm² thus resulting in the remarkably large cross section in Figure 16.

Table 11: Results: Heavy Ions at UCL - Calculated cross sections Calculated with the formulae in ESCC25100 with CL=0.95 and flux uncertainty of 10% (approx. worst case)

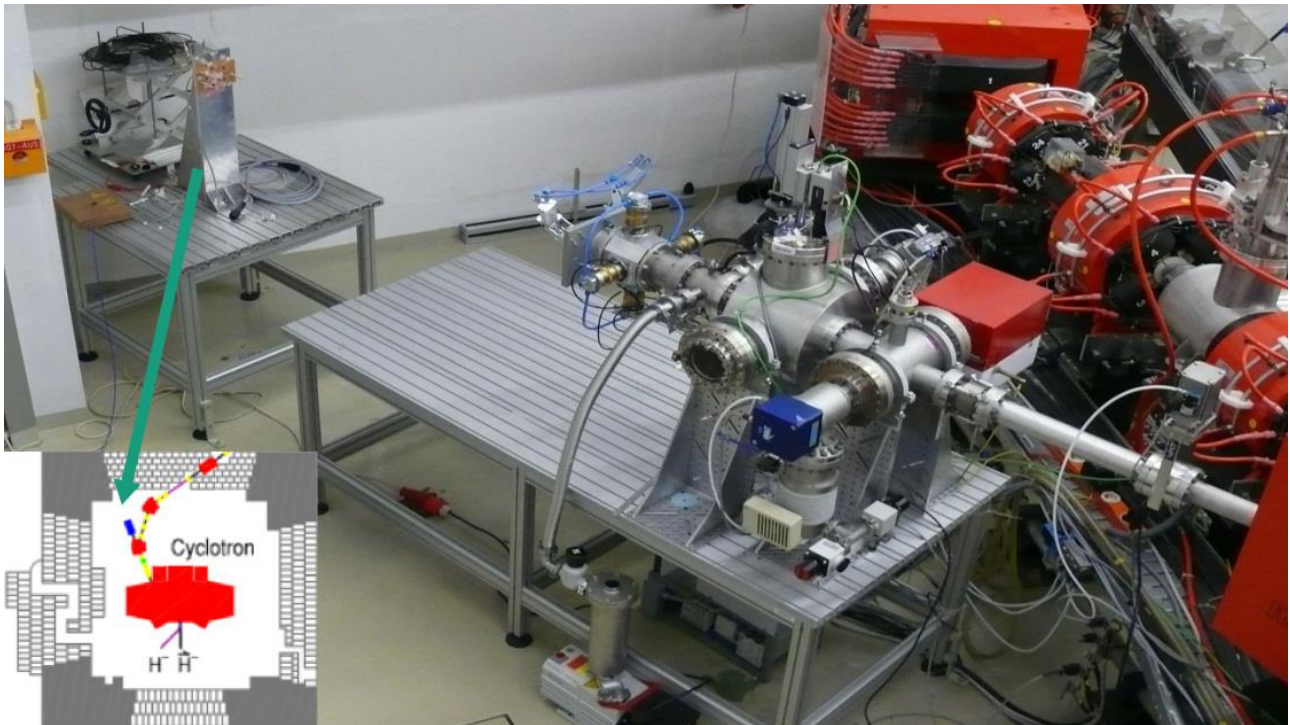
#	Ion	DUT #	V	Failure fluence [cm ⁻²]	σ lower [cm ²]	σ [cm ²]	σ upper [cm ²]	Effect	Comment
111	Al	16.2	600	2.99e+04	3.26e-05	3.35e-05	1.53e-04	FAIL	Destructive failure at indicated fluence
112	Al	15.1	500	1.01e+05	0	0	3.66e-05	--	--
113	Al	15.1	550	3.10e+05	0	0	1.19e-05	--	Run#113 was stopped after a fluence of 1.02E+05 cm ⁻² for a post test which the device passed. Slight continuous increase of leakage current observed
114	Al	15.1	550					--	
115	Al	15.2	550	3.09e+05	0	0	1.19e-05	--	Slight continuous increase of leakage current observed
116	C	15.2	600	3.05e+05	0	0	1.21e-05	--	--
117	C	15.2	750	3.08e+05	0	0	1.20e-05	--	--
118	C	15.2	900	3.11e+05	0	0	1.19e-05	--	--
119	C	15.2	1050	3.08e+05	0	0	1.20e-05	--	--
120	C	15.2	1200	3.06e+05	0	0	1.21e-05	--	--
121	C	16.1	1200	3.08e+05	0	0	1.20e-05	--	One Event with jump in leakage current observed
122	Kr	16.1	100	1.01e+05	0	0	3.65e-05	--	--
123	Kr	16.1	200	1.01e+05	0	0	3.65e-05	--	None
124	Kr	16.1	300	1.01e+05	0	0	3.66e-05	--	Pronounced continuous increase of leakage current
125	Kr	15.1	250	3.08e+05	0	0	1.20e-05	--	Run#113 was stopped after a fluence of 1.02E+05 cm ⁻² for a post test which the device passed.
126	Kr	15.1	250					--	
127	Kr	15.2	250	3.02e+05	0	0	1.22e-05	--	None
128	Cr	20.1	300	1.03e+05	0	0	3.59e-05	--	None
129	Cr	20.1	400	1.04e+05	0	0	3.56e-05	--	Pronounced continuous increase of leakage current
130	Cr	20.2	350	3.12e+05	0	0	1.17959E-05	--	Run#130 was stopped after a fluence of 1.03E+05 cm ⁻² for a post test which the device passed. Pronounced continuous increase of leakage current
131	Cr	20.2	350					--	
132	Cr	17.1	300	3.08e+05	0	0	1.20e-05	--	None
133	Cr	17.1	600	2.76e+02	0	0	2.02e-02	--	Destructive failure at indicated fluence

6 Tests at JULIC

6.1 Facility

Proton tests were performed at the JULIC injector cyclotron of the Forschungszentrum Jülich (FZJ, Research Centre Jülich). JULIC is the injector cyclotron of the Cooler Synchrotron COSY.

Figure 17: Beam line and irradiation site at the JULIC injector cyclotron, FZ Jülich



The initial energy of the proton beam is fixed to 45.0 MeV inside the cyclotron (vacuum). Usually the device under test (DUT) is placed at 1.8 m distance from the exit window of the beam. After passing the exit window of 1 mm aluminium and the air the mean proton energy is reduced to 39.3 MeV at the surface of DUT (Figure 18 and Figure 19). The maximum current of the beam is 10 μA (i.e. $6.24 \cdot 10^{13}$ p+/s). The beam has a Gaussian profile with a FWHM of about 7 cm at the surface of the DUTs.

The dose is measured online with Farmer Ionisation Chambers 30010 (measurement volume of 0.6 cm³) from PTW and an electrometer Multidos T10004 from PTW. Typically this type of ionisation chamber (IC) is used as an absolute dose-meter in high energy photon, electron, or proton-radiation therapy. The ionisation chambers are calibrated with a Co-60 gamma reference field against national standards by the manufacturer. The PMMA cap of the chamber further reduces the energy to 30.5 MeV inside the chamber.

The dose D given by the IC is related to the particle fluence Φ by the linear energy transfer (LET):

$$D = \frac{1}{\rho} \cdot \frac{dE}{dx} \cdot \Phi$$

LET

The conversion factor is obtained by a numerical simulation by MULASSIS (Geant4). For the experimental setup a fluence $\Phi = 10^{10} \text{ p}^+/\text{cm}^2$ at the exit window produces a dose $D = 24.38(15) \text{ Gy}(\text{air})$ in the ionization chamber. Alternatively, the LET (also called stopping power) of protons in different materials can be looked up at [11].

Figure 18: Schematic setup of the beam exit window at JULIC and the ionization chamber. The DUT is placed in same distance as the IC.

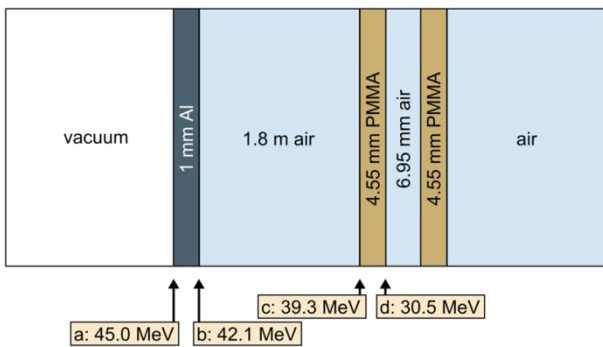
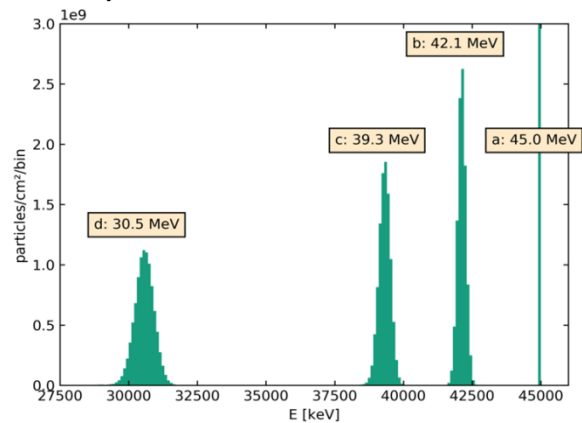


Figure 19: The initial proton energy of 45.0 MeV gets reduced to 39.3 MeV at the position of the IC/DUT. The PMMA cap of the chamber further reduces the energy to 30.5 MeV, calculation by MULASSIS (Geant4) on SPENVIS[10].



For the current tests, packaged Silicon Carbide devices were irradiated with the protons. Thus to calculate the LET on the die, additional simulations were performed with GRAS (Geant4).

6.2 Beam parameters

To receive the impact in terms of proton energy and LET on the Silicon Carbide die with packaged DUTs, radiation transport simulations have to be made. Simulation were performed with GRAS and a combination of MULASSIS and SRIM. Details on the approach and intermediate results are given in Appendix C.1. We see more of an impact on package thickness and nearly no impact of the package material. Thus here we will give a summary of the results just by thickness of the package.

Table 12: Results of simulations of the LET with package thickness. Details on the approach and intermediate results are given in Appendix C.1

Thickness	0.5 mm		1 mm		2 mm		3 mm	
LET _{GRAS} [MeV cm ² /mg]	0.012		0.008		0.005		0.003	
LET _{SRIM} [MeV cm ² /mg]	0.013		--		--		0.016	
Atomic recoil	Silicon	Carbon	Silicon	Carbon	Silicon	Carbon	Silicon	Carbon
Peak LET _{SRIM} [MeV cm ² /mg] at max. recoil	12.30	5.81	12.16	5.81	11.86	5.80	11.31	5.80
Range [μm]	2.01	6.6	1.96	6.3	1.84	5.7	1.72	5.1

While the results from GRAS and SRIM are not identical, the proton induced LET is well below 0.02 MeV cm²/mg in any case. The LETs of the recoil nuclei in SiC vary strongly with the LET of Si at or below 12.3 MeV cm²/mg and the LET of C around 5.8 MeV cm²/mg. For the overall data evaluation we identify the proton data with an LET of 0.01 MeV cm²/mg.

The thickness of the actual aluminum lid of the DUTs is around 0.5 - 1 mm.

6.3 Geometry

The DUT was positioned off-center from the beam, such that all ionization chambers and the DUT position are at the same distance from the center, thus allowing to calculate the proton flux at the DUT position without a fixed installation at the facility which would allow to do that. As a drawback, only one DUT position on the board could be used at a time. The beam still was incident normally (90°) to the surface of the DUT.

6.4 Irradiation steps

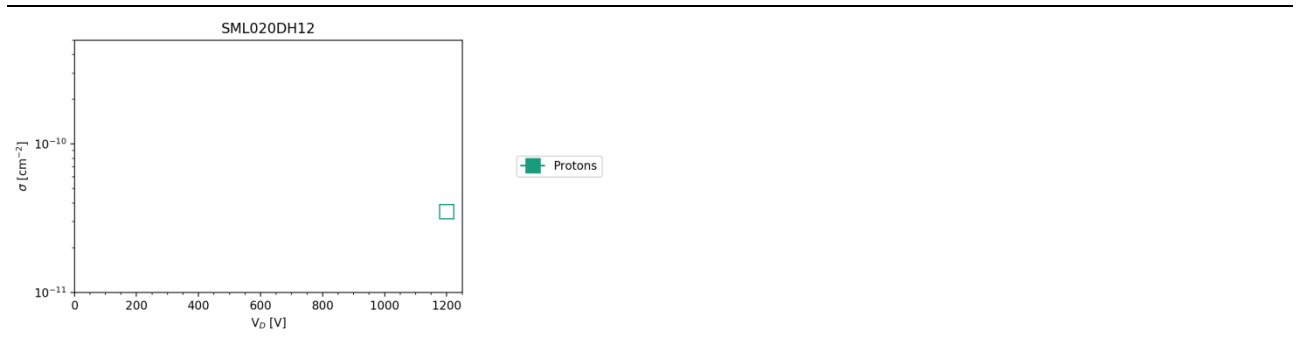
The log file of the tests performed at JULIC can be found in Appendix C. Table 13 shows an overview over the test indicating pass and fail results. A detailed evaluation of the results is shown in Section 6.5

Table 13: JULIC: Irradiation steps of SiC Schottky Diode SML020DH12. Numbers indicate the DUT serial number from Table 4. Table cells without numbers indicate that no run was performed under these conditions. Green or red background color indicate PASS or FAIL respectively. If a DUT fails at some voltage, all higher voltages are also indicated as fail. Yellow color (if applicable) indicates mixed results (e.g. 1 DUT passing, 1 DUT failing at the same level) or non-conclusive results with the device showing some damage not clearly attributable to a fail.

V _R [V]	Proton	
	E _{init} = 45 MEV	
	in-situ	POST
1200	1.1, 1.2, 2.1	1.2, 2.1

6.5 Results

Figure 20: Overview of results: Protons at JULIC. The test at 1200 V was verified with 3 diodes (in 2 packages). Filled symbols mark the cross section in case of device failures and error bars mark the upper lower limits. Open symbols mark the cross section upper limit in case no failure was observed during a run.



Tests with this device were verified with 3 diodes at 1200 V and a fluence of approx. 1e11 p/cm² per run. In the heavy ion tests with carbon (LET = 1.3 MeV cm²/mg) in Section 5, the DUTs of this device already passed tests at 1200 V.

Table 14: Results: Heavy Ions at UCL - Calculated cross sections Calculated with the formulae in ESCC25100 with CL=0.95 and flux uncertainty of 10% (approx. worst case)

#	Ion	DUT #	V _{DS} , V	Failure fluence [cm-2]	σ lower [cm2]	σ [cm2]	σ upper [cm2]	Effect	Comment
42	p	1.1	1200	1.05E+11	0	0	3.5E-11	--	--
43	p	1.2	1200	1.05E+11	0	0	3.51E-11	--	--
44	p	2.1	1200	1.05E+11	0	0	3.51E-11	--	--

7 Tests at GANIL

7.1 Facility

GANIL offers the irradiation of electric components with heavy ions over a wide LET range.

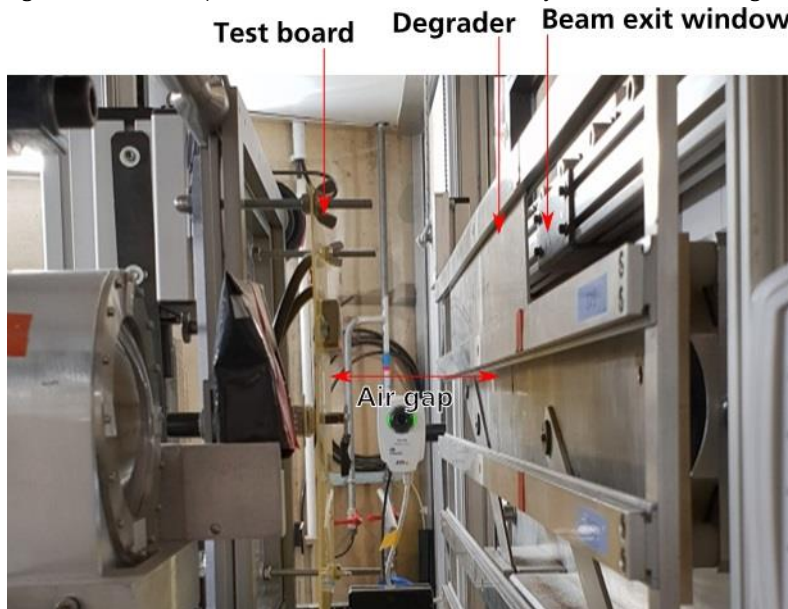
Additional heavy ion tests were performed at the G4 cave at GANIL, Caen, France.

The facility can provide selected heavy ion beams from Argon to Lead with a larger kinetic energy per nucleon than is available e.g. at UCL. The available ion at the time of our tests was Xenon.

The experimental tests at the facility take place in air and the setup consists of a sample holder, which is moveable in x-,y- and z-direction and variable degraders that can be put between the beam exit window and the DUT. By inclusion or variation of the degrader and by varying the air gap between exit window and DUT, the LET in Silicon can be tuned from approx. 26.5 MeV cm²/mg to 64.3 MeV cm²/mg and the corresponding ranges of the ions in Silicon go from 685 μm to 35 μm over that LET range.

DUT aligned is done with the help of a laser system.

Figure 21: Test setup at GANIL. Ion LETs can be set by variation of the degrader and the air gap.



7.2 Beam parameters

The resulting total energies of the respective ions, as well as their LET and range in Silicon are provided by GANIL [12]. However this data is not valid for Silicon Carbide.

SRIM 2013 [9] simulations by Fraunhofer INT in Table 15 show the respective values for the Xenon beam provided by GANIL under normal incidence in Silicon Carbide covered by a 10 μm Parylene layer with the air gap and degrader settings used in the experiments. For comparison, the values in Silicon provided by GANIL are included in the table. The devices used for these tests were de-lidded, so packages were not included in the simulations.

Table 15: GANIL: Beam characteristics. Values in Silicon are provided by GANIL [12], Values in SiC are calculated by INT

Degrader [mm Al]	Air gap [mm]	LET (Si) (MeV.cm ² /mg)	Range (Si) [μm]	LET _{SURF} (SiC) [MeV.cm ² /mg]	Range (SiC) [μm]
0	150	27.76	640.33	29.2	430
0.4	95	42.03	226.23	47.2	141
0.5	180	60.12	65.68	72.9	30

7.3 Geometry

The board is attached to the moveable board holder (Figure 21). Tests are then performed in air.

7.4 Irradiation steps

The log file of the tests performed at GANIL can be found in Appendix D. Table 16 shows an overview over the test indicating pass and fail results. A detailed evaluation of the results is shown in Section 7.5.

Table 16: GANIL: Irradiation steps of SiC Schottky Diode SML020DH12. Numbers indicate the DUT serial number from Table 4. Table cells without numbers indicate that no run was performed under these conditions. Green or red background color indicate PASS or FAIL respectively. If a DUT fails at some voltage, all higher voltages are also indicated as fail. Yellow color (if applicable) indicates mixed results (e.g. 1 DUT passing, 1 DUT failing at the same level) or non-conclusive results with the device showing some damage not clearly attributable to a fail.

		Xe, 0 mm Al, 150 mm Air		Xe, 0.4 mm Al, 95 mm Air		Xe, 0.5 mm Al, 180 mm Air	
V_DS [V]	V_GS [V]	29.2		47.2		72.9	
		in-situ	PIGS	in-situ	PIGS	in-situ	PIGS
150	0					21.2	
200				19.2, 21.1	19.2, 21.1	21.1	21.1
250		18.1, 18.2, 19.1	18.1, 18.2, 19.1	19.2	19.2		
300		18.1	18.1				

7.5 Results

The device (nominally) passed the tests during irradiation, although some damage can be seen in form of quasi-continuous device degradation. However during the PIGS test the currents increased by approx. one order of magnitude.

From the tests at UCL we could already anticipate destructive effects at fairly low voltages with the LETs at GANIL. Thus in these tests, the diode voltage was not increased beyond 250 V. No destructive events were observed, but a quasi-continuous degradation was already present.

Figure 22: Results: Protons at GANIL. The cross section results for various settings of V_{DS} . Filled symbols mark the cross section in case of device failures and error bars mark the upper lower limits. Open symbols mark the cross section upper limit in case no failure was observed during a run. No destructive effects were observed during the irradiations.

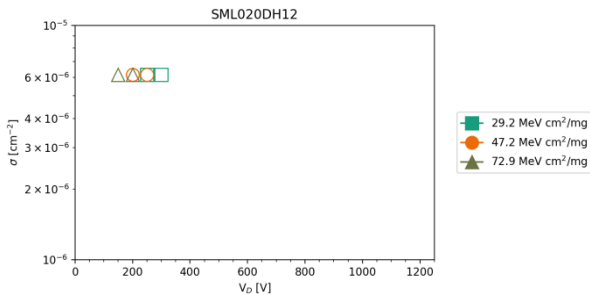


Table 17: Results: Heavy Ions at GANIL - Calculated cross sections Calculated with the formulae in ESCC25100 with $CL=0.95$ and flux uncertainty of 10% (approx. worst case)

#	Ion	Al [μm]	Air [mm]	DUT #	V_{DS} , V	Failure fluence [cm ⁻²]	σ lower [cm ²]	σ [cm ²]	σ upper [cm ²]	Effect	Comment
125	Xe	0	150	18.1	250	6.00E+05	0	0	6.15E-06	--	No dominant effect observable. DUT fails PIGS.
126	Xe	0	150	18.1	300	6.00E+05	0	0	6.15E-06	Degr.	Constant degradation. DUT fails PIGS test.
127	Xe	0	150	18.2	250	6.00E+05	0	0	6.15E-06	Degr.	Constant degradation. DUT fails PIGS test.
128	Xe	0	150	19.1	250	6.00E+05	0	0	6.15E-06	Degr.	Constant degradation. DUT fails PIGS test.
129	Xe	400	95	19.2	200	6.00E+05	0	0	6.15E-06	--	--
130	Xe	400	95	19.2	250	6.00E+05	0	0	6.15E-06	Degr.	Constant degradation. DUT fails PIGS test.
131	Xe	400	95	21.1	200	6.00E+05	0	0	6.15E-06	--	No effect observable. DUT fails PIGS.
132	Xe	500	180	21.1	200	6.00E+05	0	0	6.15E-06	Degr.	Constant degradation. DUT fails PIGS test.
133	Xe	500	180	21.2	150	6.00E+05	0	0	6.15E-06	--	No effect observable. No PIGS performed.

A Fraunhofer INT

A.1. About the institute

The Fraunhofer Institute for Technological Trend Analysis INT provides scientifically sound assessments and counselling on the entire spectrum of technological developments. On this basis, the Institute conducts Technology Forecasting, making possible a long-term approach to strategic research planning. Fraunhofer INT constantly applies this competence in projects tailor-made for our clients.

Over and above these skills, we run our own experimental and theoretical research on the effects of ionizing and electromagnetic radiation on electronic components, as well as on radiation detection systems. To this end, INT is equipped with the latest measurement technology. Our main laboratory and large-scale appliances are radiation sources, electromagnetic simulation facilities and detector systems that cannot be found in this combination in any other civilian body in Germany.

For more than 40 years, INT has been a reliable partner for the Federal German Ministry of Defence, which it advises in close cooperation and for which it carries out research in technology analysis and strategic planning as well as radiation effects. INT also successfully advises and conducts research for domestic and international civilian clients: both public bodies and industry, from SMEs to DAX 30 companies.

Further information can be found on the website [1].

A.2. Business unit Nuclear Effects in Electronics and Optics

The Business Unit „Nuclear Effects in Electronic and Optics (NEO)“ at Fraunhofer INT investigates the effects of ionizing radiation on electronic, optoelectronic, and photonic components and systems. Its work is based on more than 40 years of experience in that field.

NEO performs irradiation tests based on international standards and advises companies regarding radiation qualification and hardening of components and systems. The knowledge obtained in years of radiation testing is also used for the development of new radiation sensor systems. These activities are performed either at irradiation facilities installed at INT or at partner institutions to which our scientists have regular access.

A multitude of modern equipment to measure electrical and optical parameters is available. Furthermore our institute runs a precision mechanical workshop and an electronic laboratory. This enables us to conduct most of the irradiation tests without help or equipment of the customer.

The activities within NEO are:

- Investigations of the effects in all kinds of radiation environments
- Performance, analysis, and evaluation of irradiation tests done at Fraunhofer INT and external facilities

- Ensuring the operability of components and systems in typical radiation environments, such as space, nuclear facilities, medicine, or accelerators
- Consulting users and manufacturers on the use of products in radiation environments by selecting, optimizing and hardening
- Measurement of the radiation effects on optical fibers and fiber Bragg gratings (FBG)
- Development of radiation sensors based on optical fibers, FBGs, oscillating crystals, UV-EPROMs, and SRAMs
- Participation in the development of international test procedures for IEC, IEEE, NATO, and IAEA
- Since 2013 all services of the business unit are certified according to ISO 9001

A.3. Irradiation facilities

Fraunhofer INT operates several irradiation facilities on site that are dedicated to perform irradiation tests. For that purpose the design and operation characteristics are highly optimised from many decades of experience and to comply with all relevant standards and test procedures.

Furthermore Fraunhofer INT accesses regularly external facilities, partly with dedicated irradiation spots for exclusive use to Fraunhofer INT.

These irradiation facilities are:

- Co-60 irradiation sources on site to simulate the effect of total dose
- Neutron generators on site to simulate the displacement damage of heavy particles
- 450 keV X-ray irradiation facility on site
- Laser induced single event test system on site
- Dedicated proton irradiation spot at the injector cyclotron of FZ Jülich to simulate the effects of solar and trapped protons
- External Co-60 irradiation sources for high dose and high dose rate irradiations

The facilities used in the context of this work will be described in detail in the following sections.

A.4. QM-Certificate



MANAGEMENT SYSTEM CERTIFICATE

Certificate No: 126306-2012-AQ-GER-DAKKS	Initial certification date: 13. February 2013	Valid: 14. February 2019 - 12. February 2022
---	--	---

This is to certify that the management system of



**Fraunhofer-Institut für
Naturwissenschaftlich-Technische
Trendanalysen INT**
Appelsgarten 2, 53879 Euskirchen, Germany

has been found to conform to the Quality Management System standard:

ISO 9001:2015

This certificate is valid for the following scope:

**Scientific research on the effects of nuclear and electromagnetic radiation
as well as application and development of methods for their characterization**

Place and date:
Essen, 14. February 2019



For the issuing office:
DNV GL - Business Assurance
Schnieringshof 14, 45329 Essen, Germany


Thomas Beck
Technical Manager

Lack of fulfillment of conditions as set out in the Certification Agreement may render this Certificate invalid.
ACCREDITED UNIT: DNV GL Business Assurance Zertifizierung und Umweltgutachter GmbH, Schnieringshof 14, 45329 Essen, Germany.
TEL: +49 201 7296-222. www.dnvgl.de/assurance

B Appendix: Tests at UCL

B.1. Logfile / Test steps

In case of device failure the fluences in this table indicate the fluence provided by the facility not the fluence until failure which may differ by some additional seconds of beam.

#	Run (UCL)	Date	Time	Ion	Device Type	Device	Position on board	DUT #	V	beam time [s]	fluence [cm-2]
111	139	17.04.	23:02	Al	Schottky	SML020DH12	#1	16.2	600	380	7.10E+04
112	140	17.04.	23:12	Al	Schottky	SML020DH12	#2	15.1	500	308	1.01E+05
113	141	17.04.	23:22	Al	Schottky	SML020DH12	#2	15.1	550	206	1.02E+05
114	142	17.04.	23:32	Al	Schottky	SML020DH12	#2	15.1	550	41	2.08E+05
115	143	17.04.	23:35	Al	Schottky	SML020DH12	#2	15.2	550	61	3.09E+05
116	144	17.04.	0:21	C	Schottky	SML020DH12	#2	15.2	600	61	3.05E+05
117	145	17.04.	0:24	C	Schottky	SML020DH12	#2	15.2	750	62	3.08E+05
118	146	17.04.	0:27	C	Schottky	SML020DH12	#2	15.2	900	175	3.11E+05
119	147	17.04.	0:32	C	Schottky	SML020DH12	#2	15.2	1050	107	3.08E+05
120	148	17.04.	0:35	C	Schottky	SML020DH12	#2	15.2	1200	142	3.06E+05
121	149	17.04.	0:39	C	Schottky	SML020DH12	#1	16.1	1200	61	3.08E+05
122	150	17.04.	0:51	Kr	Schottky	SML020DH12	#1	16.1	100	253	1.01E+05
123	151	17.04.	0:58	Kr	Schottky	SML020DH12	#1	16.1	200	158	1.01E+05
124	152	17.04.	1:02	Kr	Schottky	SML020DH12	#1	16.1	300	272	1.01E+05
125	153	17.04.	1:10	Kr	Schottky	SML020DH12	#2	15.1	250	90	1.02E+05
126	154	17.04.	1:13	Kr	Schottky	SML020DH12	#2	15.1	250	40	2.07E+05
127	155	17.04.	1:19	Kr	Schottky	SML020DH12	#2	15.2	250	221	3.02E+05
128	156	17.04.	1:40	Cr	Schottky	SML020DH12	#2	20.1	300	68	1.03E+05
129	157	17.04.	1:43	Cr	Schottky	SML020DH12	#2	20.1	400	78	1.04E+05
130	158	17.04.	1:47	Cr	Schottky	SML020DH12	#2	20.2	350	50	1.03E+05
131	159	17.04.	1:50	Cr	Schottky	SML020DH12	#2	20.2	350	41	2.09E+05
132	160	17.04.	1:54	Cr	Schottky	SML020DH12	#1	17.1	300	61	3.08E+05
133	161	17.04.	1:57	Cr	Schottky	SML020DH12	#1	17.1	600	6	6.42E+02

B.2. Measurements

Figure 23: Run# 111, SML020DH12, Al-250, 7.1×10^4 ions/cm², DUT 16.2, $V_D = 600.0$ V

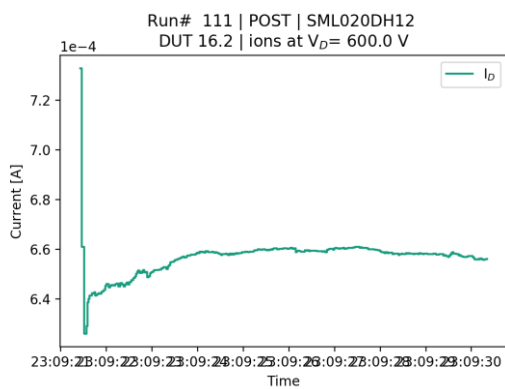
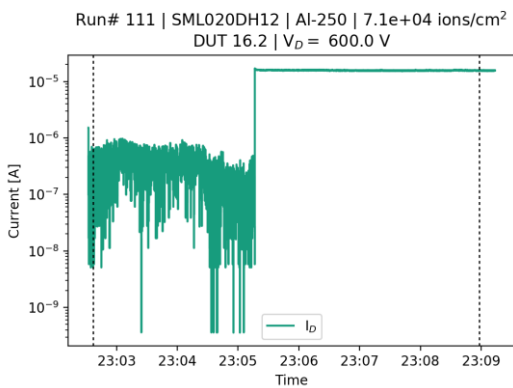
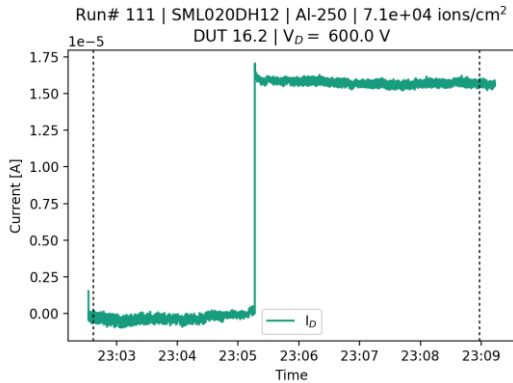


Figure 24: Run# 112, SML020DH12, Al-250, 1.0×10^5 ions/cm², DUT 15.1, $V_D = 500.0$ V

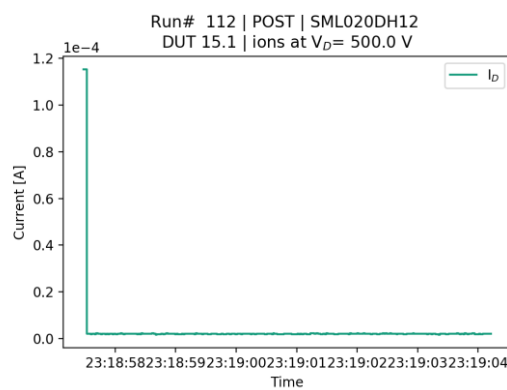
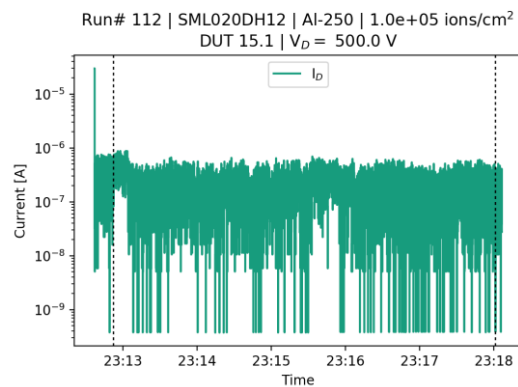
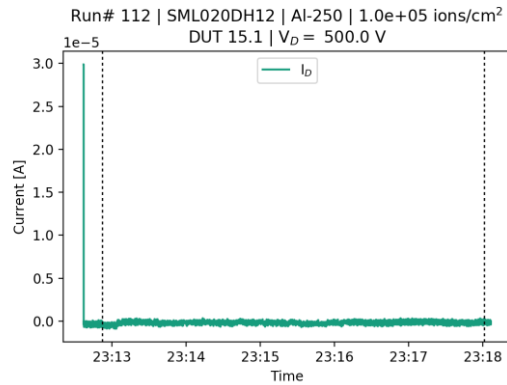


Figure 25: Run# 113, SML020DH12, Al-250, $1.0e+05$ ions/cm², DUT 15.1, $V_D = 550.0$ V

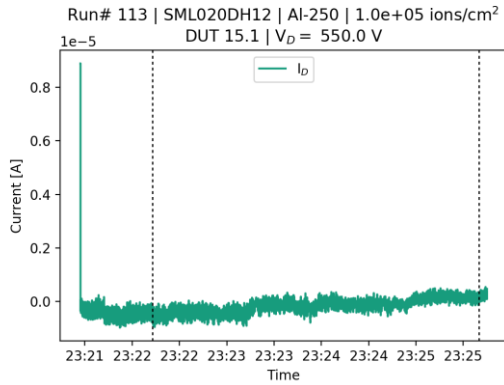


Figure 26: Run# 114, SML020DH12, Al-250, $2.1e+05$ ions/cm², DUT 15.1, $V_D = 550.0$ V

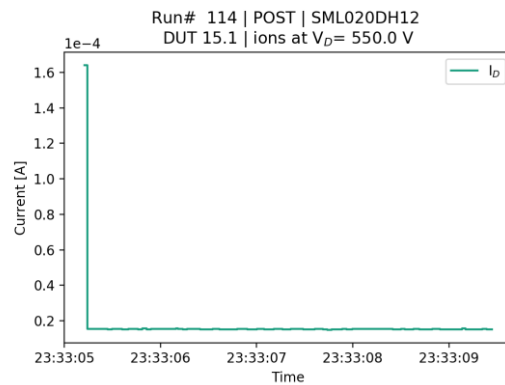
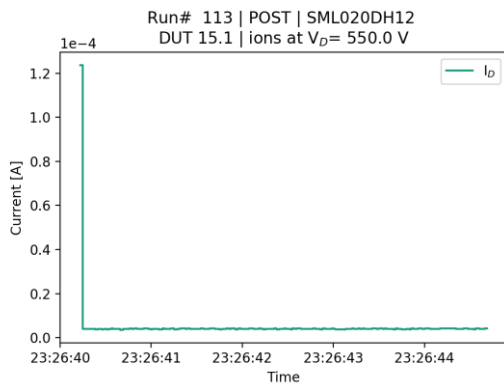
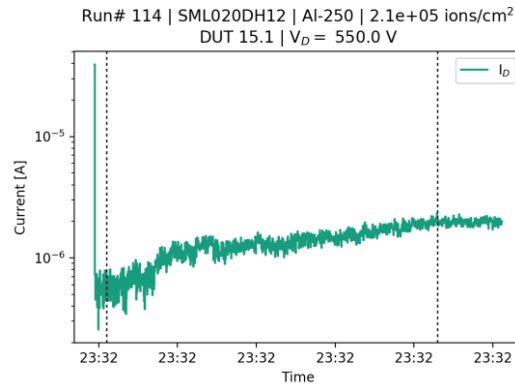
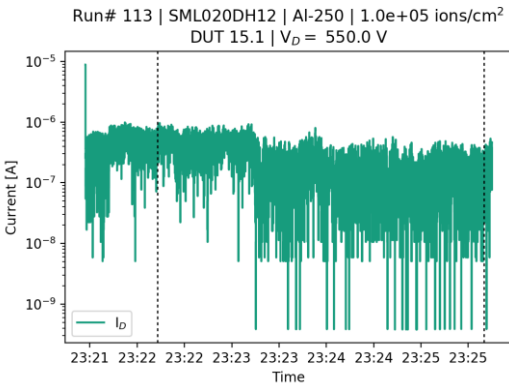
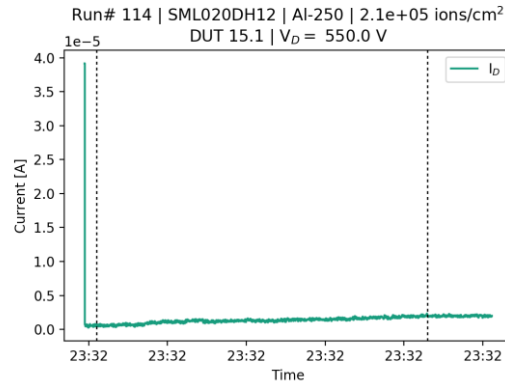


Figure 27: Run# 115, SML020DH12, Al-250, 3.1×10^5 ions/cm², DUT 15.2, $V_D = 550.0$ V

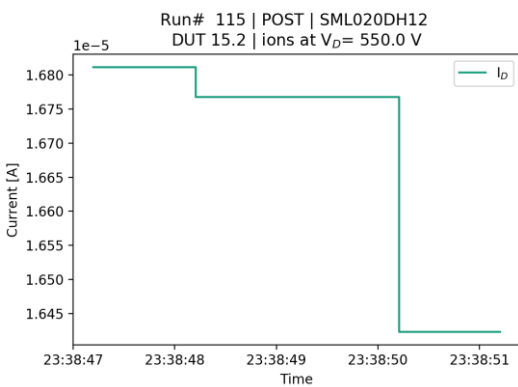
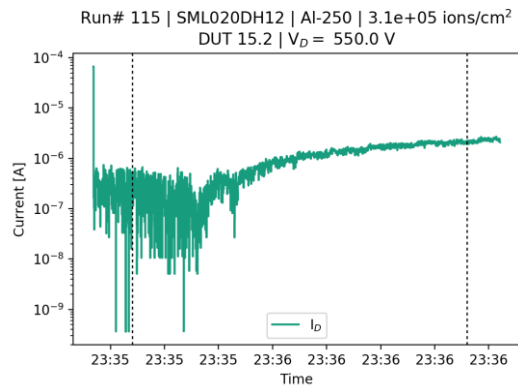
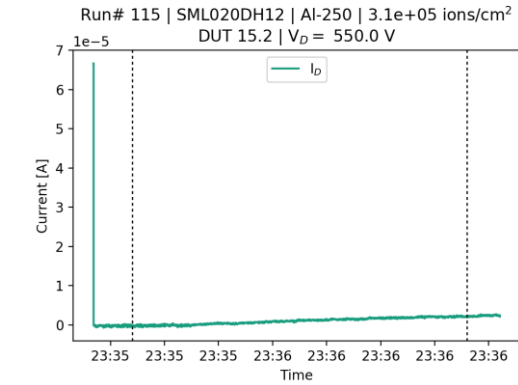


Figure 28: Run# 116, SML020DH12, C-131, 3.0×10^5 ions/cm², DUT 15.2, $V_D = 600.0$ V

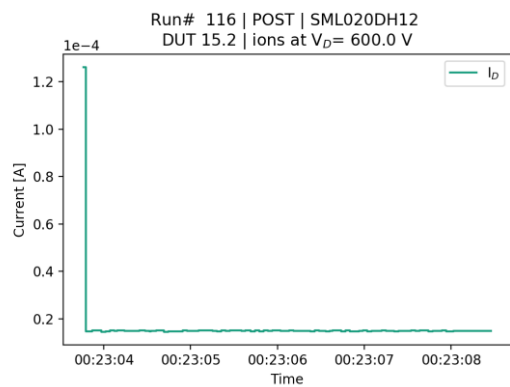
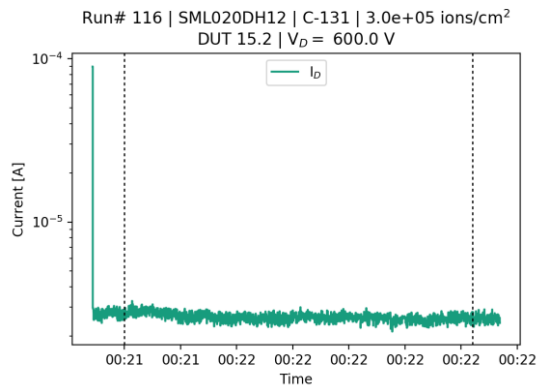
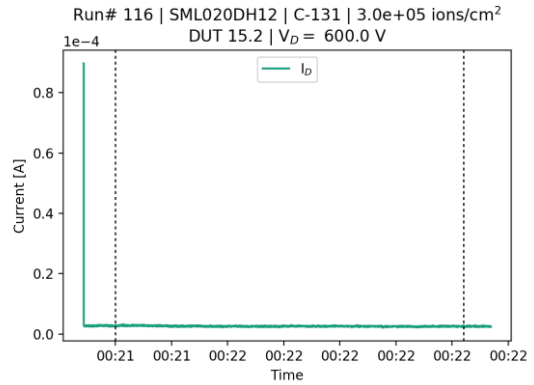


Figure 29: Run# 117, SML020DH12, C-131, 3.1×10^5 ions/cm², DUT 15.2, $V_D = 750.0$ V

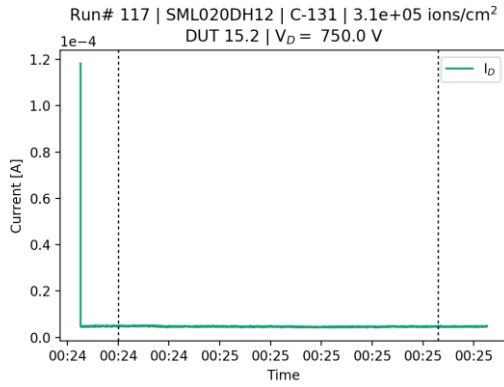


Figure 30: Run# 118, SML020DH12, C-131, 3.1×10^5 ions/cm², DUT 15.2, $V_D = 900.0$ V

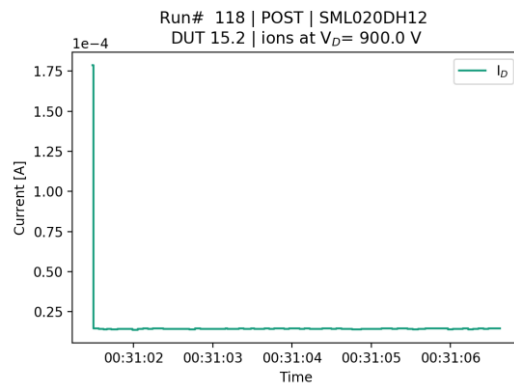
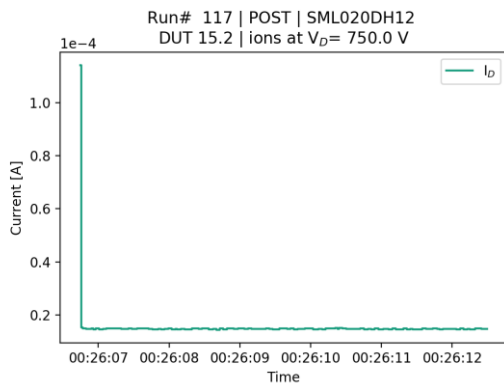
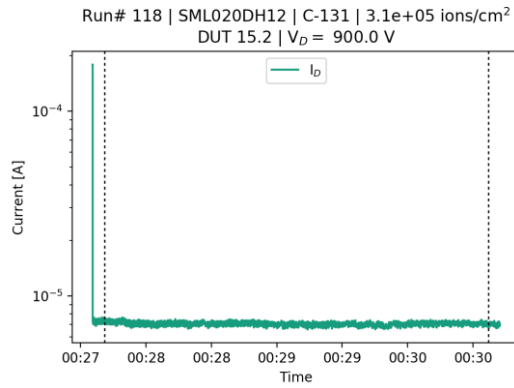
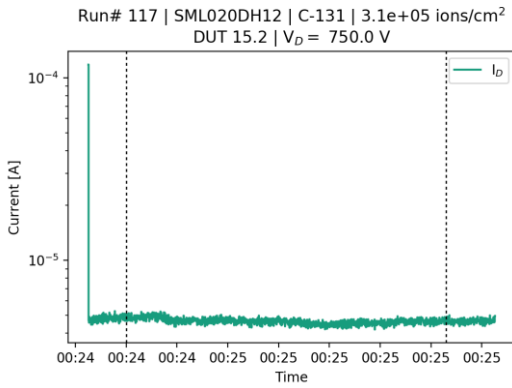
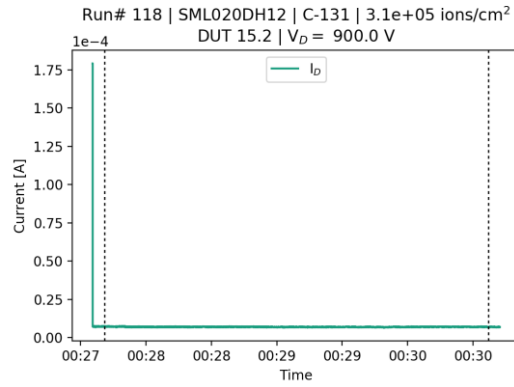


Figure 31: Run# 119, SML020DH12, C-131, 3.1×10^5 ions/cm², DUT 15.2, $V_D = 1050.0$ V

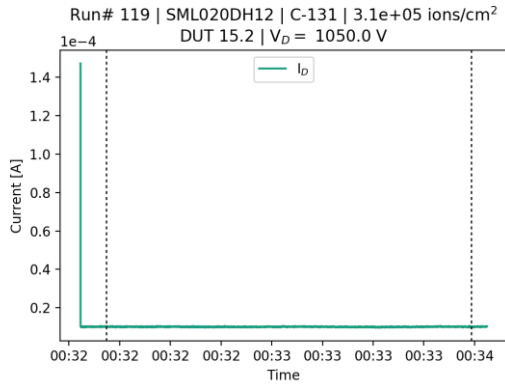


Figure 32: Run# 120, SML020DH12, C-131, 3.1×10^5 ions/cm², DUT 15.2, $V_D = 1200.0$ V

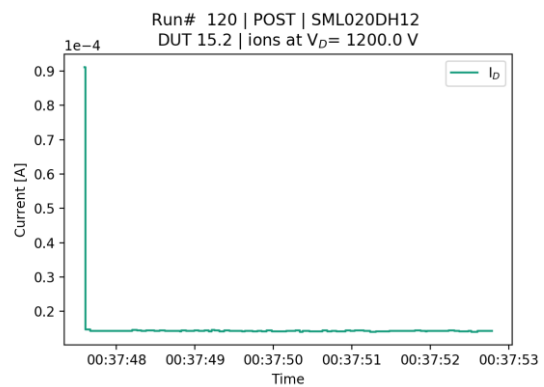
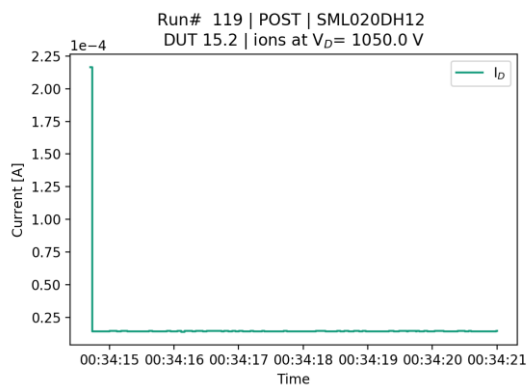
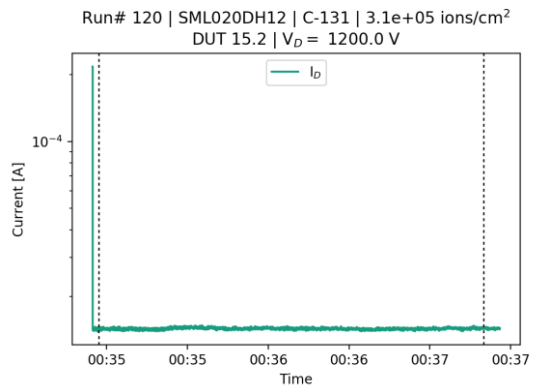
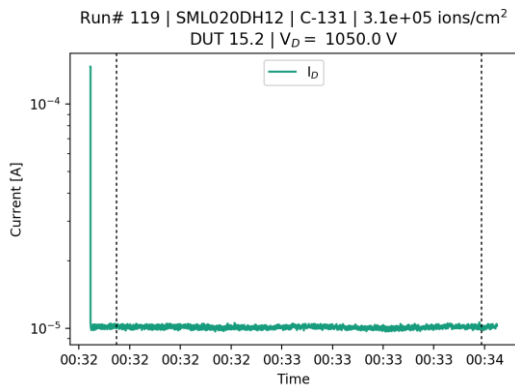
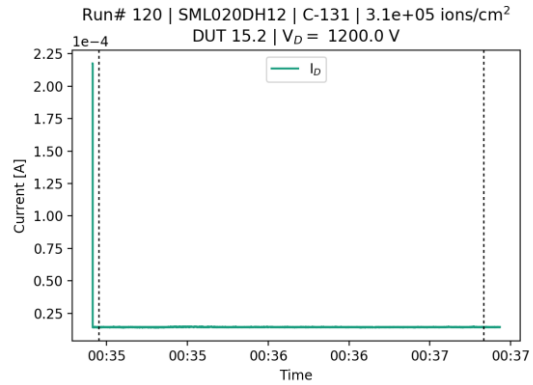


Figure 33: Run# 121, SML020DH12, C-131, 3.1×10^5 ions/cm², DUT 16.1, $V_D = 1200.0$ V

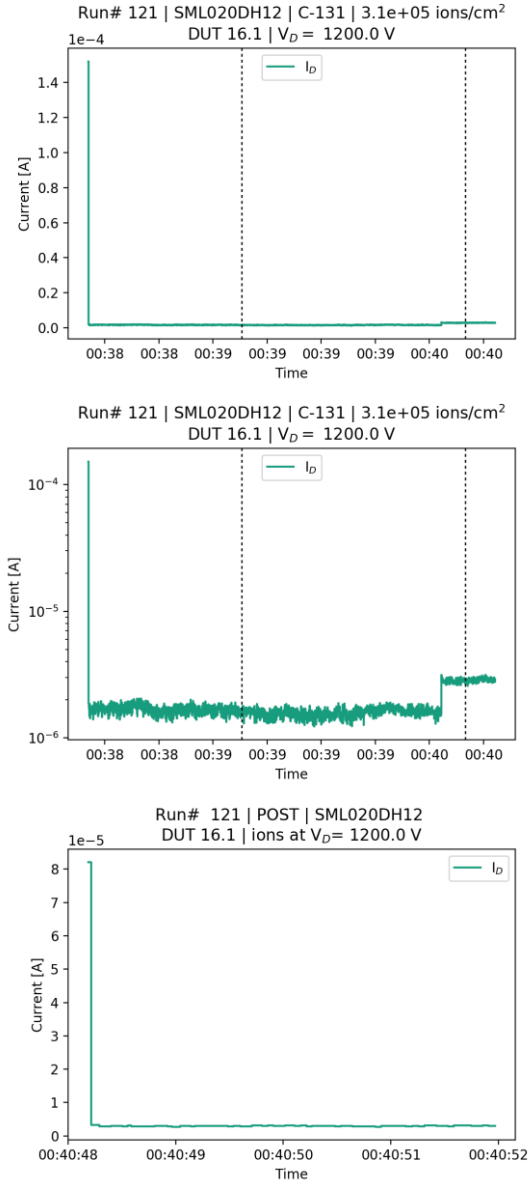


Figure 34: Run# 122, SML020DH12, Kr-769, 1.0×10^5 ions/cm², DUT 16.1, $V_D = 100.0$ V

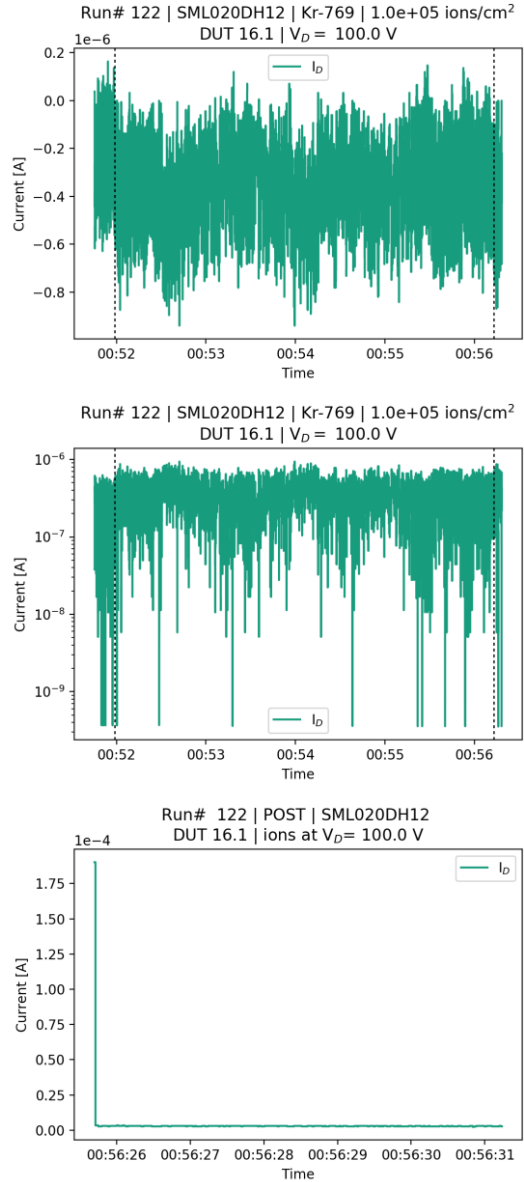


Figure 35: Run# 123, SML020DH12, Kr-769, $1.0e+05$ ions/cm², DUT 16.1, $V_D = 200.0$ V

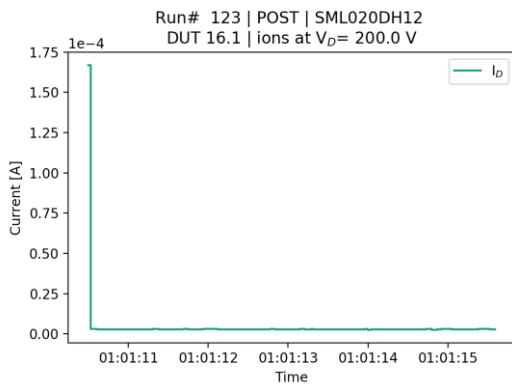
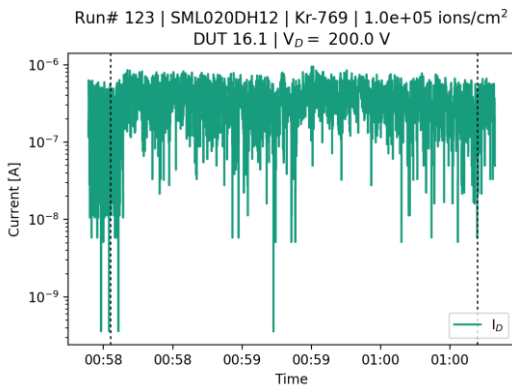
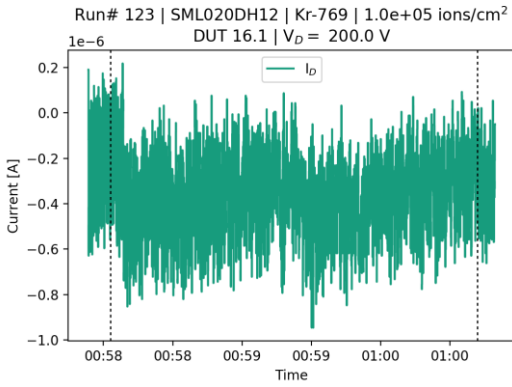


Figure 36: Run# 124, SML020DH12, Kr-769, $1.0e+05$ ions/cm², DUT 16.1, $V_D = 300.0$ V

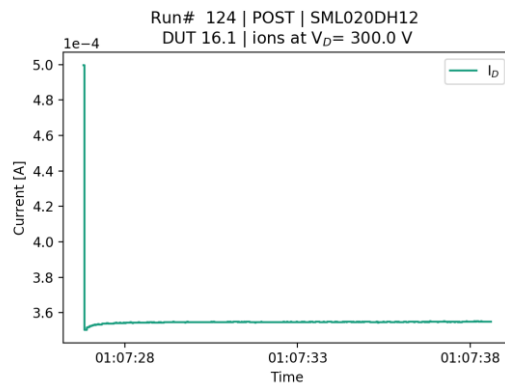
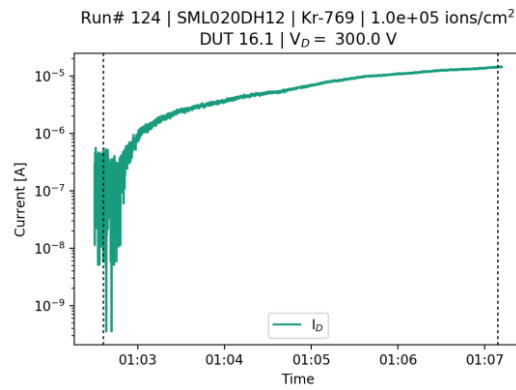
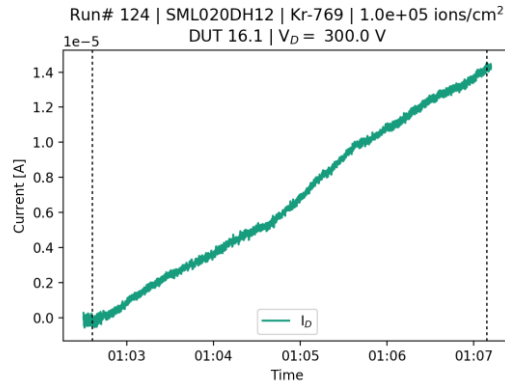


Figure 37: Run# 125, SML020DH12, Kr-769, $1.0e+05$ ions/cm², DUT 15.1, $V_D = 250.0$ V

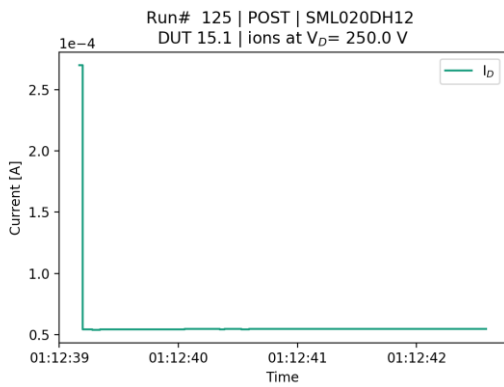
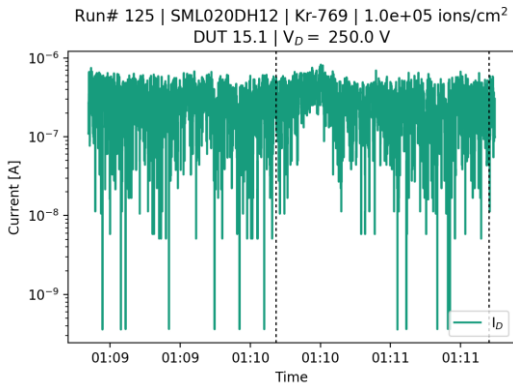
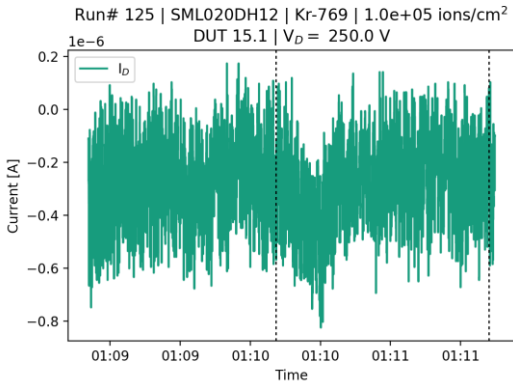


Figure 38: Run# 126, SML020DH12, Kr-769, $2.1e+05$ ions/cm², DUT 15.1, $V_D = 250.0$ V

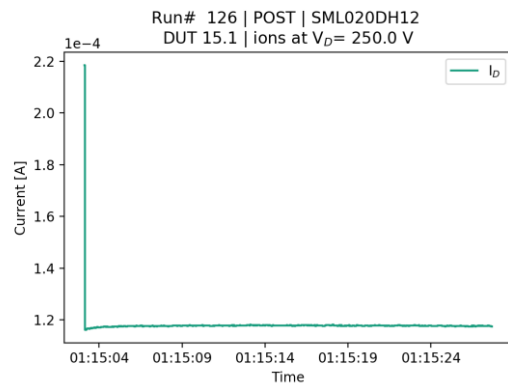
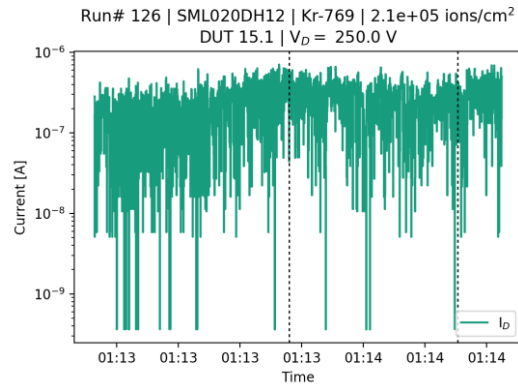
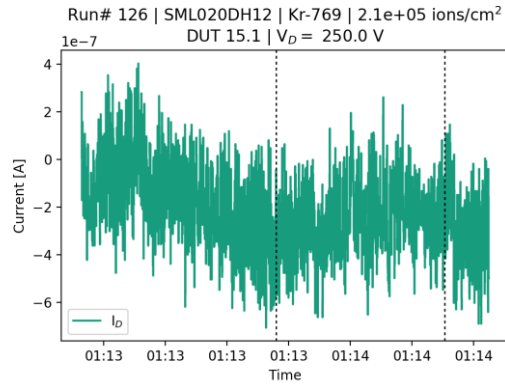


Figure 39: Run# 127, SML020DH12, Kr-769, $3.0e+05$ ions/cm², DUT 15.2, $V_D=250.0$ V

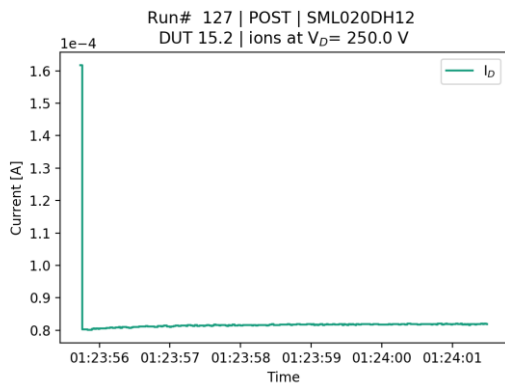
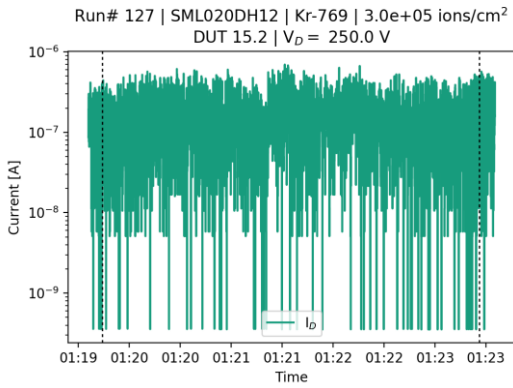
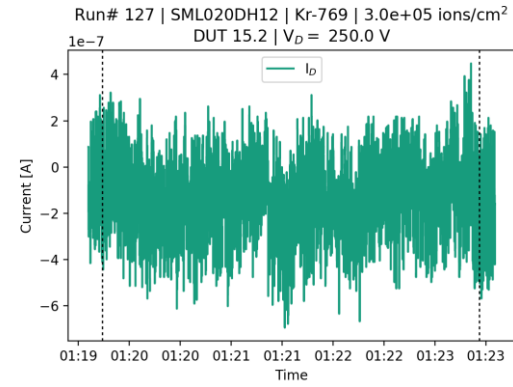


Figure 40: Run# 128, SML020DH12, Cr-513, $1.0e+05$ ions/cm², DUT 20.1, $V_D=300.0$ V

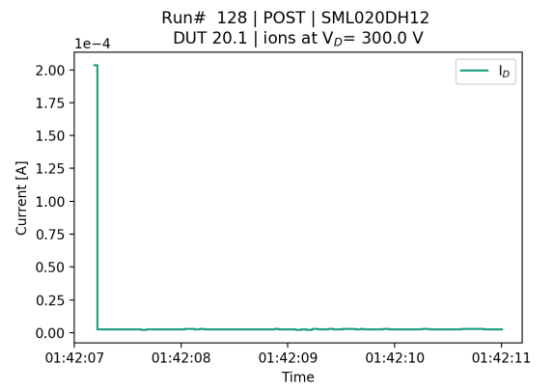
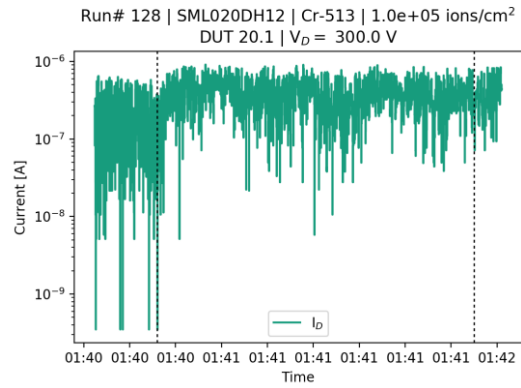
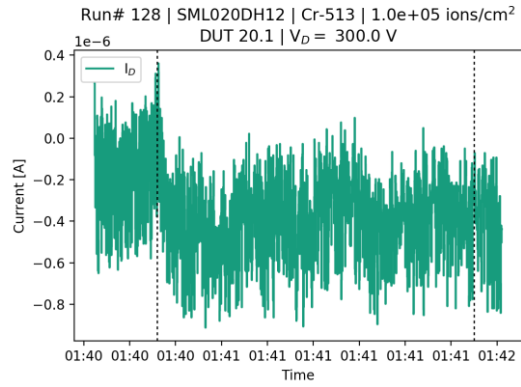


Figure 41: Run# 129, SML020DH12, Cr-513, $1.0e+05$ ions/cm², DUT 20.1, $V_D = 400.0$ V

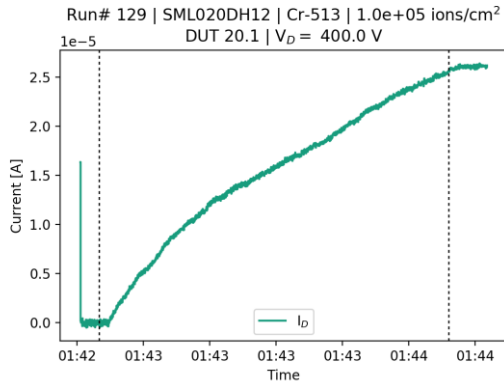


Figure 42: Run# 130, SML020DH12, Cr-513, $1.0e+05$ ions/cm², DUT 20.2, $V_D = 350.0$ V

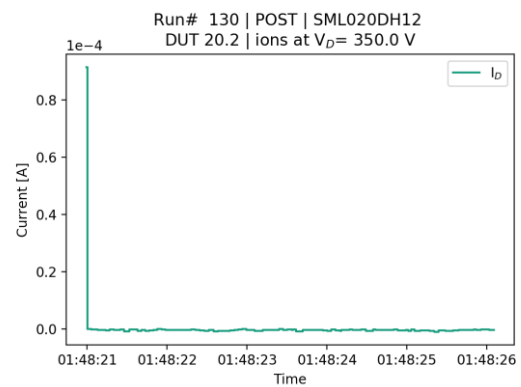
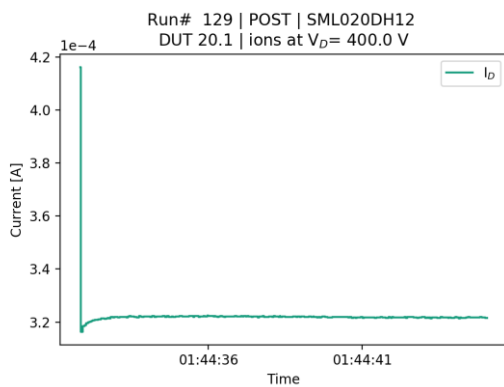
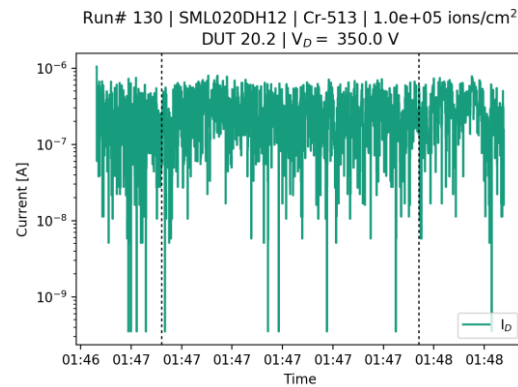
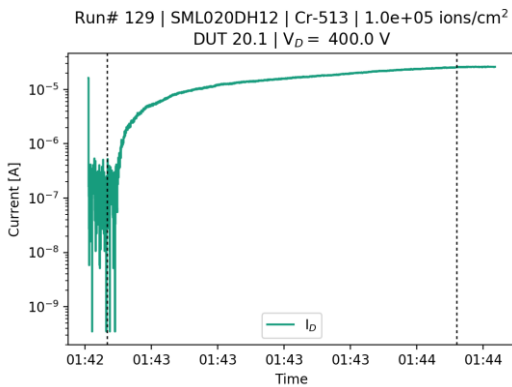
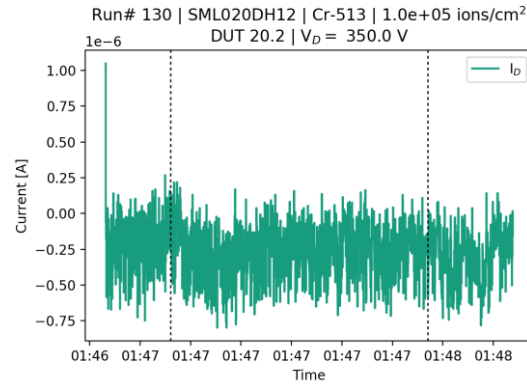


Figure 43: Run# 131, SML020DH12, Cr-513, 2.1×10^5 ions/cm², DUT 20.2, $V_D = 350.0$ V

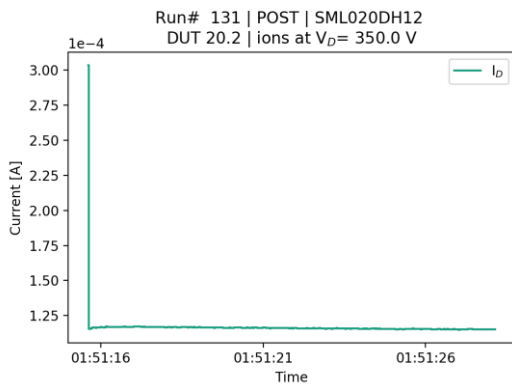
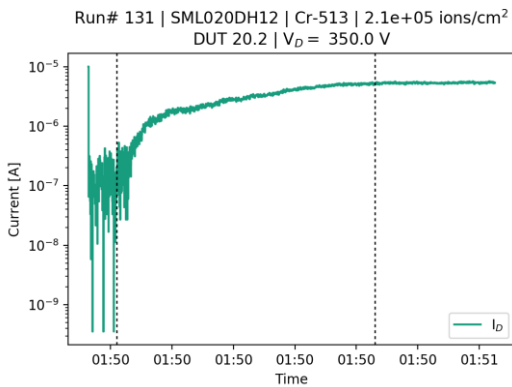
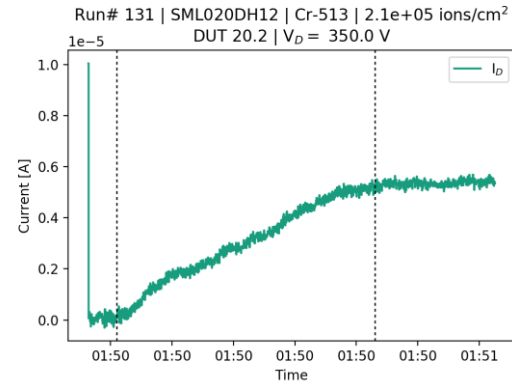


Figure 44: Run# 132, SML020DH12, Cr-513, 3.1×10^5 ions/cm², DUT 17.1, $V_D = 300.0$ V

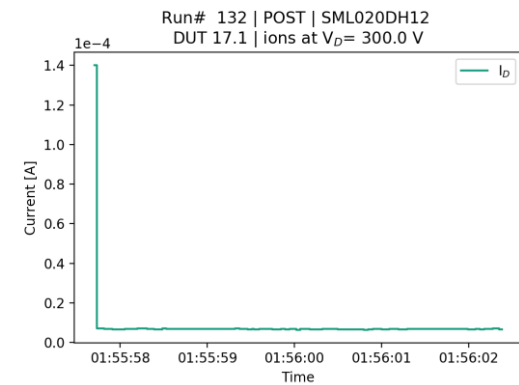
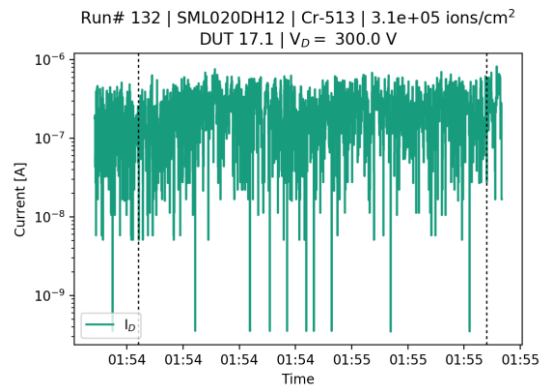
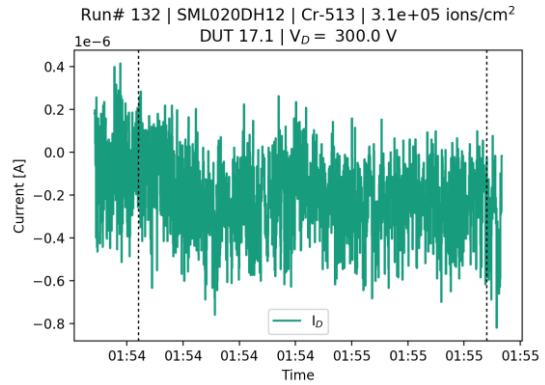
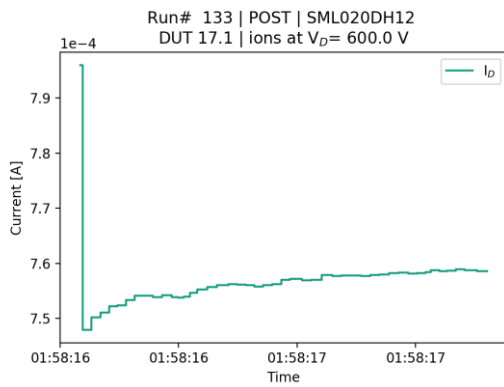
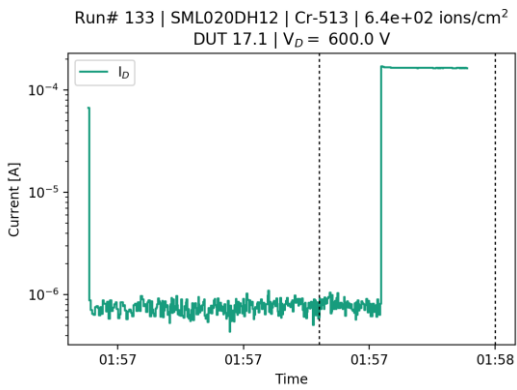
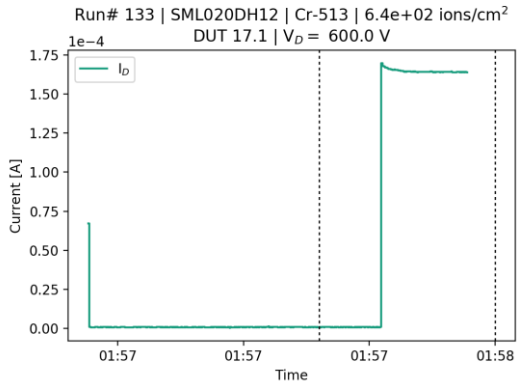


Figure 45: Run# 133, SML020DH12, Cr-513, $6.4e+02$ ions/cm², DUT 17.1, $V_D = 600.0$ V



C Appendix: Tests at JULIC

C.1. LET estimation

To receive the impact in terms of proton energy and LET on the Silicon Carbide die with packaged DUTs, radiation transport simulations have to be made:

- 1) The setup (beam exit window, air gap, package, die) were simulated with GRAS in standalone version 3.03 for $1E7$ protons. The average LET at the layer boundary from the package to the silicon carbide was evaluated by GRAS. This gives the average LET in MeV/cm. Rare events e.g. maximum recoil energy transfer, are few in these simulations. For the results in Table 12, this was then divided by the density $\rho = 3210 \text{ mg/cm}^3$ to give the LET in units of MeV cm^2/mg .
- 2) The setup (beam exit window, air gap, package, die) were simulated with MULASSIS in standalone version 1.26 for $1E7$ protons. The proton energy at the layer boundary from the package to the silicon carbide was evaluated by MULASSIS. With this proton energy, the maximum recoil energy to Silicon and Carbon atoms in SiC were calculated with $E_{ion}(E_p) = \frac{4 m_p m_{ion}}{(m_p + m_{ion})^2} \cdot E_p$. SRIM 2013 [9] simulations were then performed with the respective particles and maximum kinetic energy in Silicon Carbide. From the SRIM ionization curve the LET can then be calculated. This LET gives information on the recoils happening inside the SiC layer and is not restricted to the layer "surface" (although only extreme values were considered).

For these simulations, the 1 mm Aluminum exit window and 1.8 m of air were taken into account, such that the spread of the proton energy on the DUT package and the transport simulations through the package in the LET calculations is included. Package thickness for all materials was taken as 0.5, 1, 2 and 3 mm. The 3 mm was not simulated for Aluminum package (which was on the scale of 0.5 mm).

Alternatively the above geometry could be simulated only with SRIM. This has however some major drawbacks, when looking at a $100 \mu\text{m}$ layer at the end of the target of length $>1.8 \text{ m}$ as then only particles incident on $\pm 50 \mu\text{m}$ around the center are evaluated.

Information on the plastic package of the materials was not readily available for the use in SRIM or GRAS, as both require the atomic stoichiometry of the materials. For the sake of the Monte Carlo simulations this does not have to be chemically exact, but has to reflect the likelihood of interacting e.g. with a Silicon, if an interaction with a random nucleus takes place.

For some devices in this project, information was given in the Material Content Data Sheet. A value of 2.37 g/cm^3 was assumed for the density of the plastic mold and the stoichiometry for the example of SiC MOSFET C2M0080120D was estimated to be around Si:O:C:H = 1.6 : 3.6 : 1.2 : 1, thus the estimate for the chemical sum formula to be used in the simulations to be $\text{Si}_3\text{-O}_7\text{-C}_2\text{-H}_2$.

Table 18: Mold material of example C2M0080120D. Values indicated with * are estimates.

Name	CAS	Stoichiometry	Density [g/cm ³]	Molar mass [u]	Mass in Mold [mg]
Silicon Dioxide	7631-86-9	SiO ₂	2.6	60.0843	1640.71
Epoxy Resin	29690-82-2	C ₃₃ H ₄₂ O ₉ X ₂	1.12 *	582.68 *	189.62
Anhydride	2421-28-5	C ₁₇ H ₆ O ₇	1.57 *	322.23 *	159.68
Carbon Black	1333-86-4	C	1.7	12.01	5.99

Table 19: Results of GRAS simulations of the LET with package thickness. The GRAS results are the average "surface" LETs on the layer boundary from the package to SiC and would include error information. Error estimates are not given but are < 0.001 MeV cm²/mg in any case).

Name	LET _{GRAS} [MeV cm ² /mg]			
	0.5 mm	1 mm	2 mm	3 mm
Al	0.012	0.008	0.004	--
Si1-O2-C1-H1	0.012	0.008	0.005	0.003
Si3-O7-C2-H2	0.012	0.008	0.005	0.003
Si545-O1220-C512-H597-P3-B1	0.013	0.009	0.005	0.004

Table 20: Intermediate results of MULASSIS simulations of the proton energy with package thickness. Little variation is seen based on the package material.

Name	E(p) [MeV] at boundary Package → SiC			
	0.5 mm	1 mm	2 mm	3 mm
Al	37.72	36.08	32.64	---
Si1-O2-C1-H1	37.77	36.18	32.85	29.17
Si3-O7-C2-H2	37.80	36.24	32.97	29.38
Si545-O1220-C512-H597-P3-B1	37.77	35.75	32.83	29.15
Average	37.76	36.06	32.82	29.23
LETSRIM [MeV cm ² /mg]	0.013	--	--	0.016

Table 21: Results of SRIM simulations of the LET with package thickness. The SRIM results are the maximum LETs of the Silicon or Carbon recoil nuclei. The values given are the peak values, i.e. not necessarily at the beginning of the track, in the material. The average energies from Table 20 were taken for the recoil energies.

	Silicon				Oxygen			
	0.5 mm	1 mm	2 mm	3 mm	0.5 mm	1 mm	2 mm	3 mm
Max. Energy of Recoil Atom (180°) [MeV]	5.05	4.82	4.39	3.91	10.79	10.30	9.38	8.35
Peak LET _{SRIM} [MeV cm ² /mg] at max. recoil	12.30	12.16	11.86	11.31	5.81	5.81	5.80	5.80
Peak at track length [μm]	0	0	0	0	4.5	4.1	3.3	2.8
Range [μm]	2.01	1.96	1.84	1.72	6.6	6.3	5.7	5.1

C.2. Logfile / Test steps

In case of device failure the fluences in this table indicate the fluence provided by the facility not the fluence until failure which may differ by some additional seconds of beam.

#	Date	Time	Ion	Device Type	Device	DUT #	V_D	beam time [s]	fluence [cm ⁻²]
42	20.09.	10:24	p	MOSFET	SML020DH12	1.1	1200	259	1.1e11
43	20.09.	10:33	p	MOSFET	SML020DH12	1.2	1200	255	1.1e11
44	20.09.	10:42	p	MOSFET	SML020DH12	2.1	1200	255	1.1e11

C.3. Measurements

Figure 46: Run# 042, SML020DH12, p, 1.1e+11 p/cm², DUT 1.1, V_D= 1200.0 V

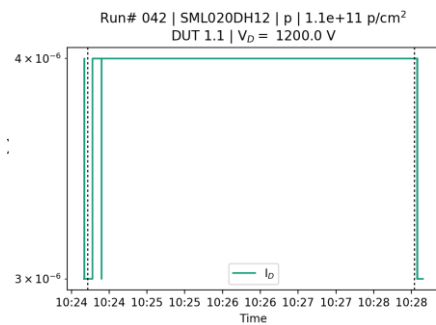
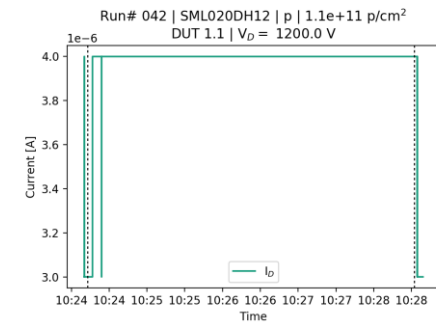
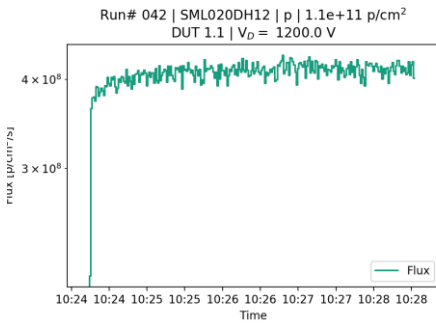


Figure 47: Run# 043, SML020DH12, p, 1.1e+11 p/cm², DUT 1.2, V_D= 1200.0 V

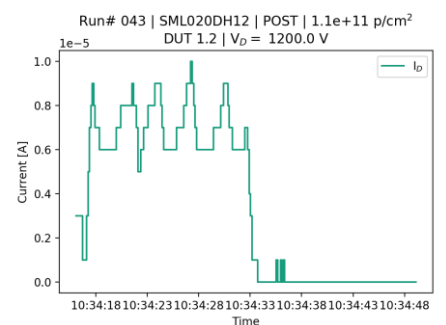
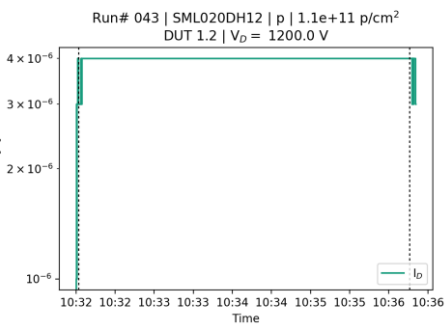
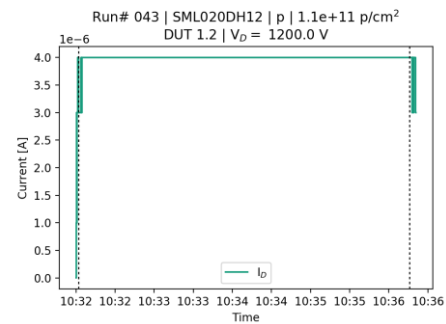
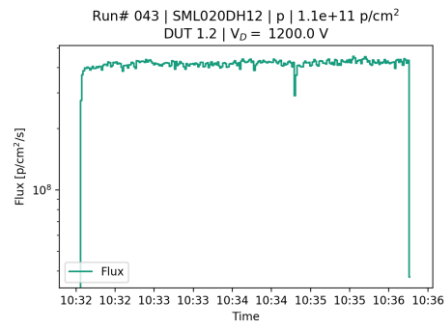
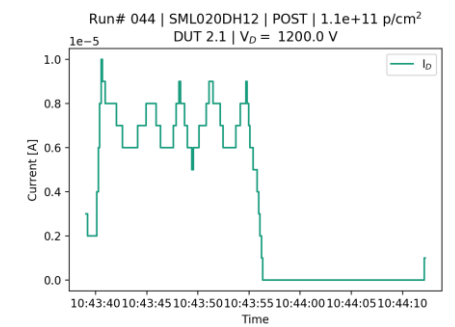
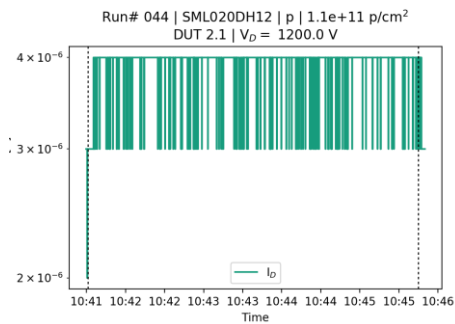
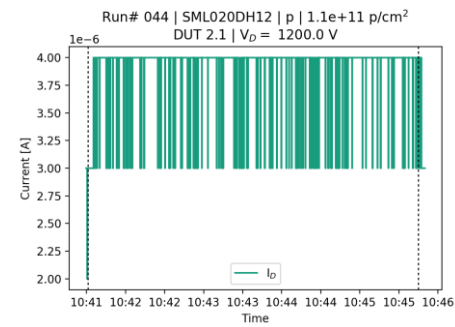
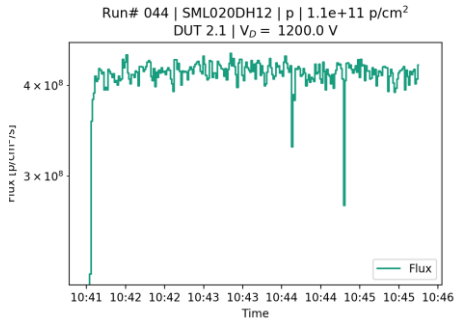


Figure 48: Run# 044, SML020DH12, p, 1.1e+11 p/cm², DUT 2.1, VD= 1200.0 V



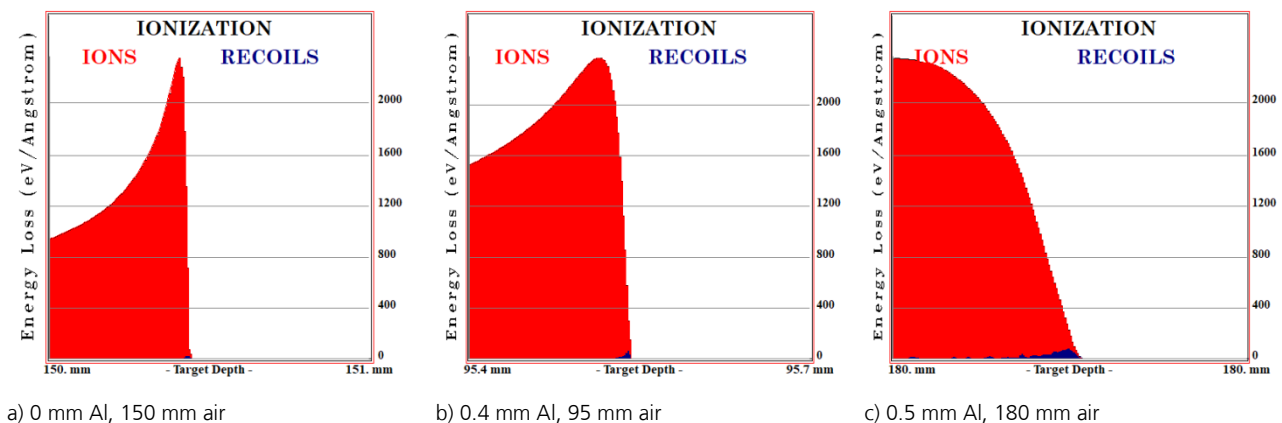
D Appendix: Tests at GANIL

D.1. LET estimation

To receive the impact in terms of LET on the Silicon Carbide die, radiation transport simulations have to be made. A major difference to the proton LET estimations, is that the tests were performed on decapsulated devices, so the package is not taken into account.

For these simulations, the 10 μm stainless steel exit window, a variable amount of air gap, and if applicable an Aluminum degrader was included in simulations with SRIM2013. The incident particles were 49.1 MeV/n Xenon ions (isotope mass = 136 u).

Figure 49: SRIM2013 simulations of the Ganil Xenon tests on SiC



The views of the ionization curves in Figure 49 start at the surface of the silicon carbide layer, so e.g. at 95.410 mm in Figure 49 b), although only one digit is displayed.

The LET in $\text{MeV cm}^2/\text{mg}$ can be directly calculated from the Energy loss in $\text{eV}/\text{\AA}$ by unit conversion ($1 \text{ eV}/\text{\AA} = 100 \text{ MeV}/\text{cm}$) and division by the SiC density of $3.21 \text{ g}/\text{cm}^3 = 3210 \text{ mg}/\text{cm}^3$.

Table 22: GANIL: Beam characteristics. Values in Silicon are provided by GANIL [12] **Fehler! Verweisquelle konnte nicht gefunden werden.**, Values in SiC are calculated by INT and given with one digit

Degrader [mm Al]	Air gap [mm]	LET (Si) ($\text{MeV}\cdot\text{cm}^2/\text{mg}$)	Range (Si) [μm]	LET _{SURF} (SiC) [$\text{MeV}\cdot\text{cm}^2/\text{mg}$]	Range (SiC) [μm]
0	150	27.76	640.33	29.2	430
0.4	95	42.03	226.23	47.2	141
0.5	180	60.12	65.68	72.9	30

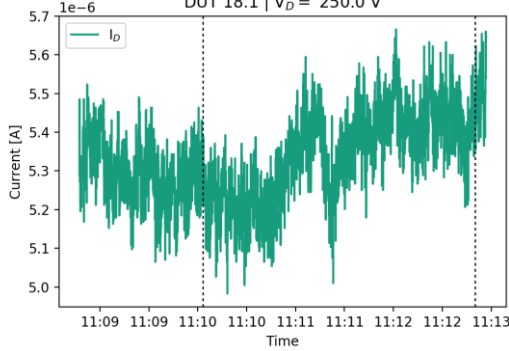
D.2. Logfile / Test steps

#	Date	Time	Ion	Al [μm]	Air [mm]	Device Type	Device	Position on board	DUT #	V_DS, V	beam time [s]	fluence [cm^{-2}]
125	06.06.	11:07	Xe	0	150	Schottky	SML020DH12	#1	18.1	250	167	6.00E+05
126	06.06.	11:12	Xe	0	150	Schottky	SML020DH12	#1	18.1	300	139	6.00E+05
127	06.06.	11:17	Xe	0	150	Schottky	SML020DH12	#1	18.2	250	159	6.00E+05
128	06.06.	11:21	Xe	0	150	Schottky	SML020DH12	#2	19.1	250	132	6.00E+05
129	06.06.	11:26	Xe	400	95	Schottky	SML020DH12	#2	19.2	200	129	6.00E+05
130	06.06.	11:29	Xe	400	95	Schottky	SML020DH12	#2	19.2	250	132	6.00E+05
131	06.06.	11:34	Xe	400	95	Schottky	SML020DH12	#3	21.1	200	130	6.00E+05
132	06.06.	11:38	Xe	500	180	Schottky	SML020DH12	#3	21.1	200	123	6.00E+05
133	06.06.	11:42	Xe	500	180	Schottky	SML020DH12	#3	21.2	150	127	6.00E+05

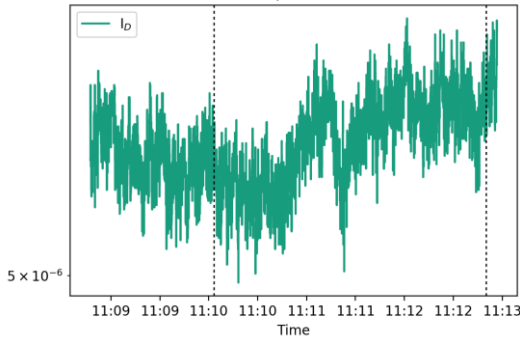
D.3. Measurements

Figure 50: Run# 125, SML020DH12, Xe 0 mmAl, 150 mm Air, $6.0e+05$ ions/cm², DUT 18.1, $V_D=250.0$ V

Run# 125 | SML020DH12 | Xe 0 mmAl, 150 mm Air | $6.0e+05$ ions/crr
DUT 18.1 | $V_D=250.0$ V



Run# 125 | SML020DH12 | Xe 0 mmAl, 150 mm Air | $6.0e+05$ ions/crr
DUT 18.1 | $V_D=250.0$ V



Run# 125 | POST | SML020DH12
DUT 18.1 | ions at $V_D=250.0$ V

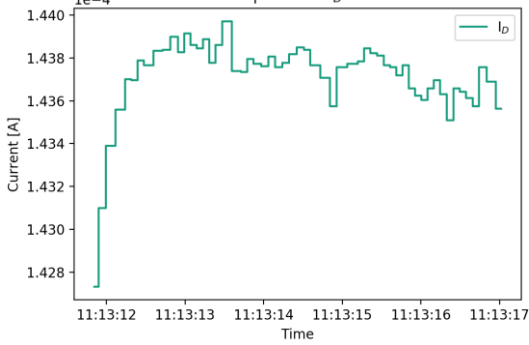
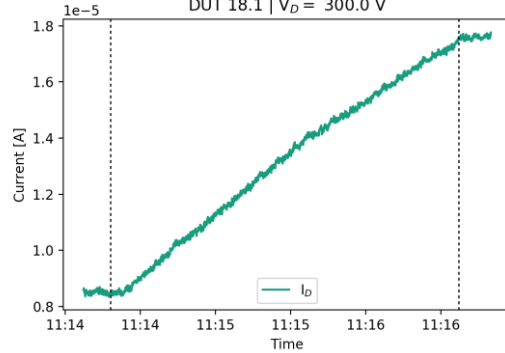
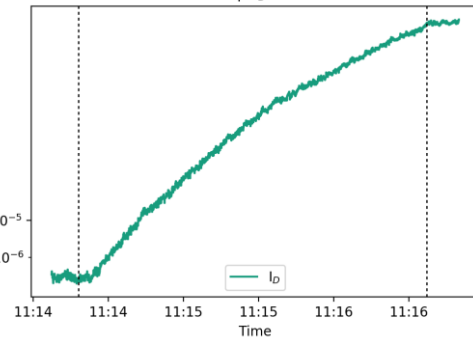


Figure 51: Run# 126, SML020DH12, Xe 0 mmAl, 150 mm Air, $6.0e+05$ ions/cm², DUT 18.1, $V_D=300.0$ V

Run# 126 | SML020DH12 | Xe 0 mmAl, 150 mm Air | $6.0e+05$ ions/crr
DUT 18.1 | $V_D=300.0$ V



Run# 126 | SML020DH12 | Xe 0 mmAl, 150 mm Air | $6.0e+05$ ions/crr
DUT 18.1 | $V_D=300.0$ V



Run# 126 | POST | SML020DH12
DUT 18.1 | ions at $V_D=300.0$ V

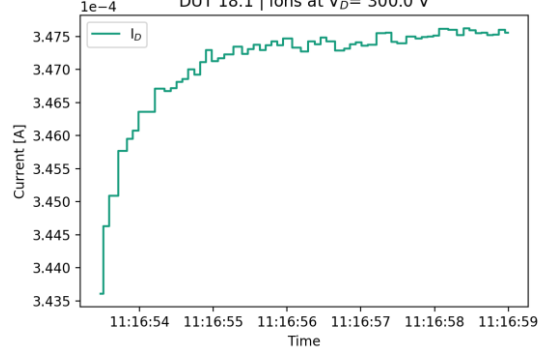
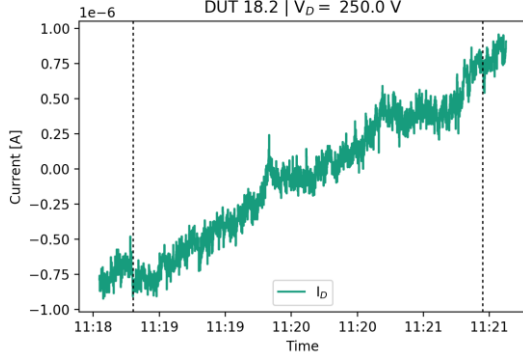


Figure 52: Run# 127, SML020DH12, Xe 0 mmAl, 150 mm Air, $6.0e+05$ ions/cm², DUT 18.2, $V_D=250.0$ V

Run# 127 | SML020DH12 | Xe 0 mmAl, 150 mm Air | $6.0e+05$ ions/cr
DUT 18.2 | $V_D=250.0$ V



Run# 127 | SML020DH12 | Xe 0 mmAl, 150 mm Air | $6.0e+05$ ions/cr
DUT 18.2 | $V_D=250.0$ V

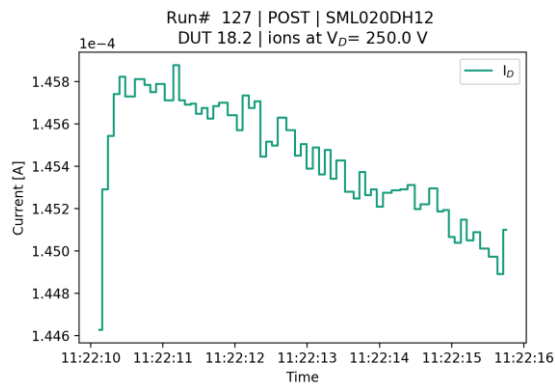
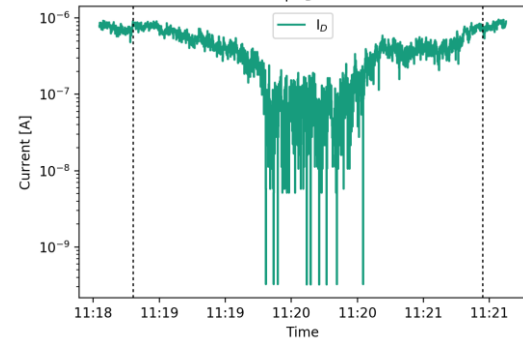
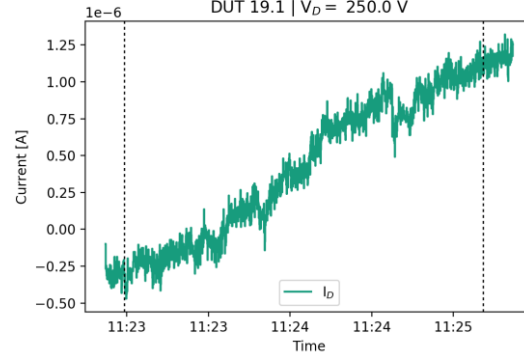


Figure 53: Run# 128, SML020DH12, Xe 0 mmAl, 150 mm Air, $6.0e+05$ ions/cm², DUT 19.1, $V_D=250.0$ V

Run# 128 | SML020DH12 | Xe 0 mmAl, 150 mm Air | $6.0e+05$ ions/cr
DUT 19.1 | $V_D=250.0$ V



Run# 128 | SML020DH12 | Xe 0 mmAl, 150 mm Air | $6.0e+05$ ions/cr
DUT 19.1 | $V_D=250.0$ V

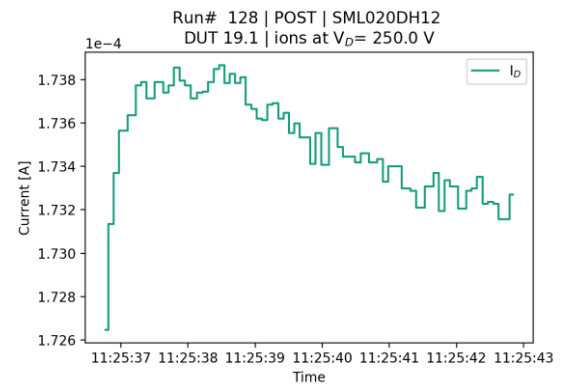
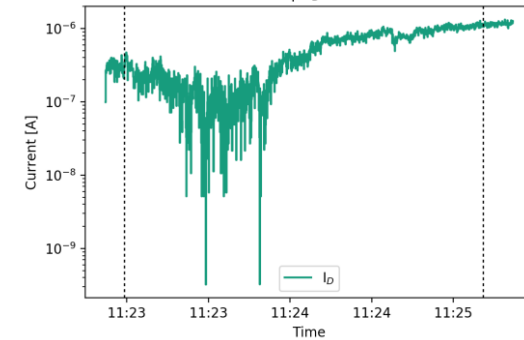
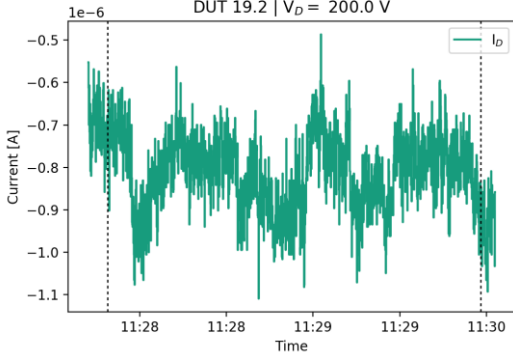
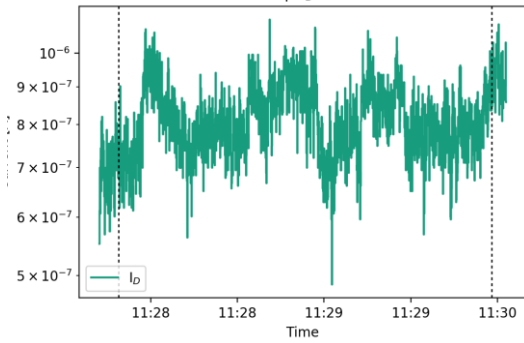


Figure 54: Run# 129, SML020DH12, Xe 400 mmAl, 95 mm Air, $6.0e+05$ ions/cm², DUT 19.2, $V_D=200.0$ V

Run# 129 | SML020DH12 | Xe 400 mmAl, 95 mm Air | $6.0e+05$ ions/cr
DUT 19.2 | $V_D=200.0$ V



Run# 129 | SML020DH12 | Xe 400 mmAl, 95 mm Air | $6.0e+05$ ions/cr
DUT 19.2 | $V_D=200.0$ V



Run# 129 | POST | SML020DH12
DUT 19.2 | ions at $V_D=200.0$ V

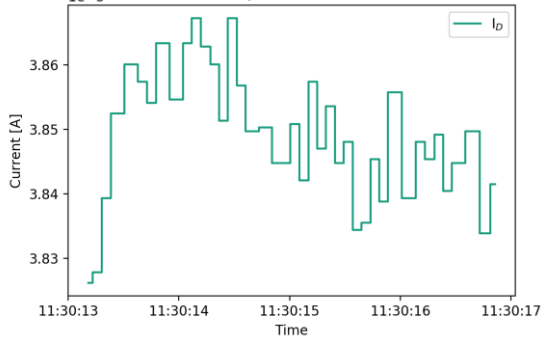
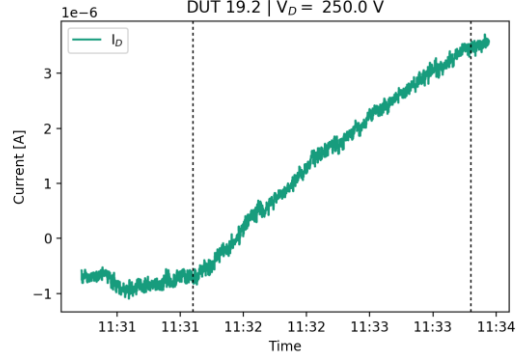
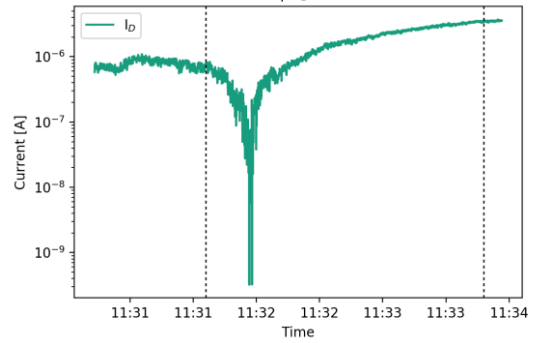


Figure 55: Run# 130, SML020DH12, Xe 400 mmAl, 95 mm Air, $6.0e+05$ ions/cm², DUT 19.2, $V_D=250.0$ V

Run# 130 | SML020DH12 | Xe 400 mmAl, 95 mm Air | $6.0e+05$ ions/cr
DUT 19.2 | $V_D=250.0$ V



Run# 130 | SML020DH12 | Xe 400 mmAl, 95 mm Air | $6.0e+05$ ions/cr
DUT 19.2 | $V_D=250.0$ V



Run# 130 | POST | SML020DH12
DUT 19.2 | ions at $V_D=250.0$ V

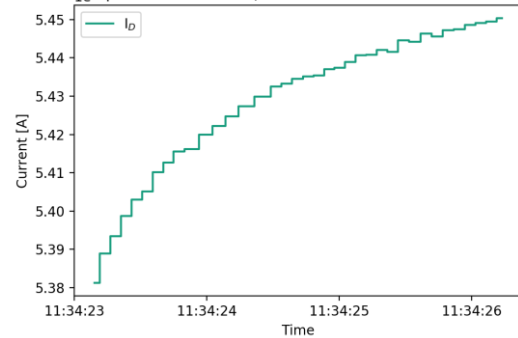
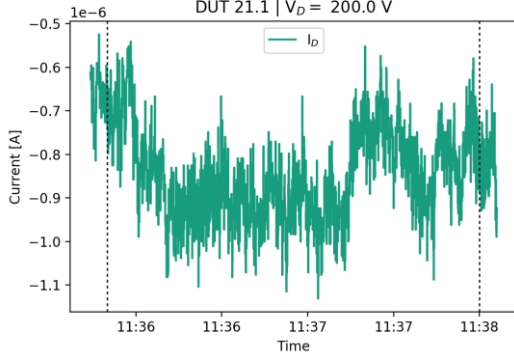
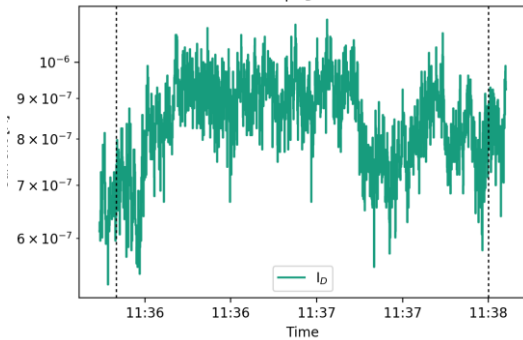


Figure 56: Run# 131, SML020DH12, Xe 400 mmAl, 95 mm Air, $6.0e+05$ ions/cm², DUT 21.1, $V_D=200.0$ V

Run# 131 | SML020DH12 | Xe 400 mmAl, 95 mm Air | $6.0e+05$ ions/cm² | DUT 21.1 | $V_D=200.0$ V



Run# 131 | SML020DH12 | Xe 400 mmAl, 95 mm Air | $6.0e+05$ ions/cm² | DUT 21.1 | $V_D=200.0$ V



Run# 131 | POST | SML020DH12 | DUT 21.1 | ions at $V_D=200.0$ V

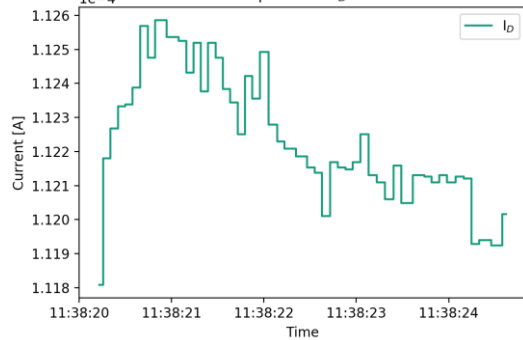
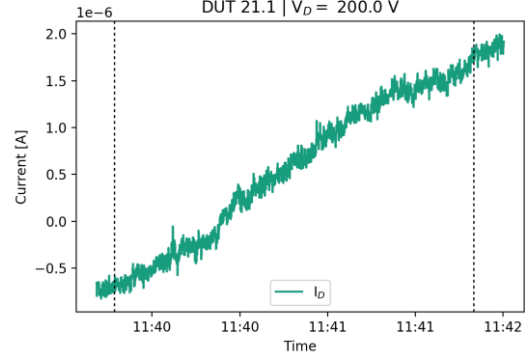
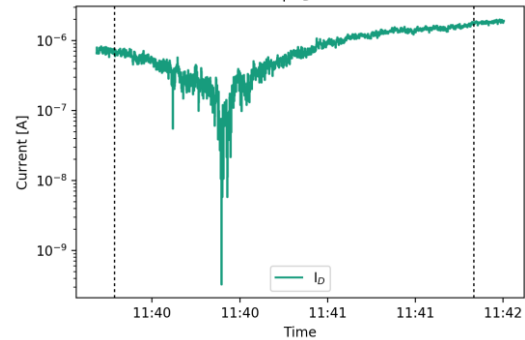


Figure 57: Run# 132, SML020DH12, Xe 500 mmAl, 180 mm Air, $6.0e+05$ ions/cm², DUT 21.1, $V_D=200.0$ V

Run# 132 | SML020DH12 | Xe 500 mmAl, 180 mm Air | $6.0e+05$ ions/cm² | DUT 21.1 | $V_D=200.0$ V



Run# 132 | SML020DH12 | Xe 500 mmAl, 180 mm Air | $6.0e+05$ ions/cm² | DUT 21.1 | $V_D=200.0$ V



Run# 132 | POST | SML020DH12 | DUT 21.1 | ions at $V_D=200.0$ V

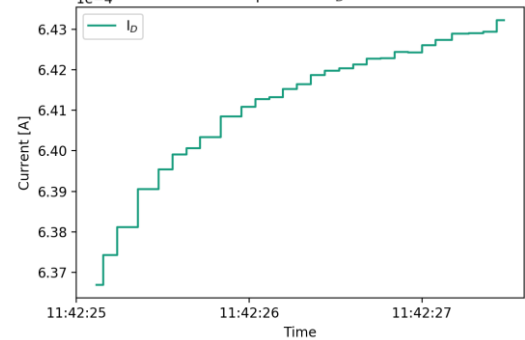
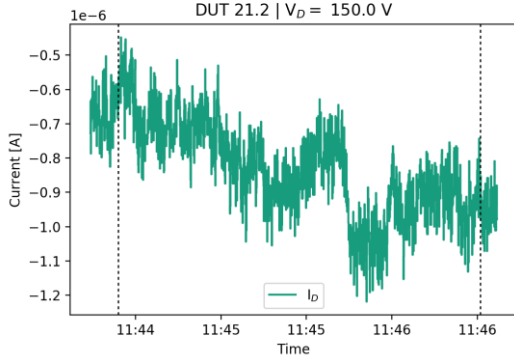


Figure 58: Run# 133, SML020DH12, Xe 500 mmAl, 180 mm Air, $6.0e+05$ ions/cm², DUT 21.2, $V_D = 150.0$ V

.un# 133 | SML020DH12 | Xe 500 mmAl, 180 mm Air | $6.0e+05$ ions/c
DUT 21.2 | $V_D = 150.0$ V



.un# 133 | SML020DH12 | Xe 500 mmAl, 180 mm Air | $6.0e+05$ ions/c
DUT 21.2 | $V_D = 150.0$ V

